

MESOSCALE PRECIPITATION PATTERNS
IN CENTRAL NEW ENGLAND

by

CHARLES KIRBY NASON

B.A., College of Wooster
(1959)



SUBMITTED IN PARTIAL FULFILLMENT
OF THE REQUIREMENTS FOR THE
DEGREE OF MASTER OF
SCIENCE
at the
MASSACHUSETTS INSTITUTE OF TECHNOLOGY
January, 1965

Signature of Author
Department of Meteorology, January 18, 1965

Certified by
Thesis Supervisor

Accepted by
Chairman, Department Committee on Graduate Students

MESOSCALE PRECIPITATION PATTERNS
IN CENTRAL NEW ENGLAND

by

CHARLES KIRBY NASON

Submitted to the Department of Meteorology on 18 January 1965
in Partial Fulfillment of the Requirements for
the Degree of Master of Science

ABSTRACT

The purpose of this study is to determine the general characteristics of mesoscale precipitation patterns in the central New England area. Sixty-four storms were selected for which the radar data clearly indicated one of three pattern types. These included 28 area patterns, 24 bands, and 12 "miscellaneous" patterns. Quantitative radar observations and hourly precipitation amounts from a network of recording rain gauges provided the basic data. In addition to the pattern type, the following quantities were computed for each storm to depict the precipitation within a radius of 80 miles from Cambridge, Massachusetts: total amount of water deposited during storm and also the maximum amount deposited within any single hour; maximum precipitation rate observed at any point; durations and dimensions of precipitation areas and bands. The characteristics of the groups were then compared.

Some of the characteristics (total amount of water deposited and maximum intensity over the 80-mile circle) were approximately the same in magnitude, while others (maximum intensity at a point, total duration of precipitation within observed area, and spatial distribution of total water) showed significant differences. The larger-scale weather systems related to the precipitation patterns were investigated, and it was found that area patterns were most often related to coastal low pressure systems and that band patterns were most often associated with cold front passage. Significant differences in the seasonal distributions of the three groups existed but because of the method of selection of the storms, little can be said about the probability that all New England storms would show the same distributions.

Thesis Supervisor: Pauline M. Austin
Title: Research Associate

ACKNOWLEDGEMENTS

The author wishes to express his appreciation to Dr. Pauline Austin for her inspiration, patience, and encouragement without which this paper would not exist.

Further acknowledgement is due to Mr. Howard Fairman for the preparation of the rain-gauge computer program and to Mr. Michael Kraus for assistance in preparing the rain-gauge maps.

Special thanks go to Mr. Steven A. Ricci for the expert preparation of the diagrams.

Finally, the author is indebted to his wife, Mrs. Patricia Nason, for the professional excellence which she brought to the task of typing his rather involved manuscript and for her never ending encouragement and patience.

TABLE OF CONTENTS

ABSTRACT	ii
ACKNOWLEDGEMENTS	iii
TABLE OF CONTENTS	iv
LIST OF FIGURES	vi
LIST OF TABLES	viii
INTRODUCTION	1
DATA AND METHODS OF ANALYSIS	5
A. Radar Measurements	5
B. Rain-Gauge Data	18
C. Comparison and Combination of Radar and Rain-gauge Data	24
D. Synoptic Data	27
E. Data Selection	29
AREAS	31
A. Intensity and Amount of Precipitation	31
B. Durations	37
C. Dimensions	42
D. Cause of Precipitation	48
E. Spatial Distribution of Total Water	51
F. Seasonal Distribution	55
BANDS	57
A. Intensity and Amount of Precipitation	57
B. Duration and Number of Bands	63
C. Band Dimensions	69
D. Cause of Precipitation	73
E. Spatial Distribution of Total Water	76
F. Special Cases	80
G. Seasonal Distribution	82

COMPARATIVE CHARACTERISTICS OF STORMS WITH PRECIPITATION AREAS, BANDS OR MISCEL- LANEOUS PATTERNS	83
A. Miscellaneous Storms	83
B. Summary of Characteristics of the Various Groups	86
C. Total Water	86
D. Intensity	88
E. Durations	89
F. Dimensions	91
G. Cause of Precipitation	91
H. Seasonal Distribution	92
CONCLUSIONS	94
REFERENCES	98

LIST OF FIGURES

Fig. 1.	Film prints of AN/CPS-9 iso-echo contours, 0530 EST, 20 March 63.	10
Fig. 2.	Digital map of intensity levels, 0530 EST, 20 March 63.	11
Fig. 3.	Theoretical and actual calibration curves.	13
Fig. 4.	Position and spread of radar beams as a function of range.	17
Fig. 5a.	Map of rain-gauge stations reporting hourly amounts in New England.	19
Fig. 5b.	Computer output showing hour rainfall amounts for 1000 EST, 10 Nov 62.	19
Fig. 5c.	Digital map of AN/CPS-9 echoes, 0910 EST, 10 Nov 62.	19
Fig. 6.	Histogram of hourly areal intensity for 19-20 Oct 60.	22
Fig. 7.	Distribution of maximum precipitation intensity at a point.	34
Fig. 8.	Distribution of maximum hourly intensity over 80-mile circle.	34
Fig. 9.	Spatial intensity distributions, 1-2 March 63	36
Fig. 10.	Durations of entire storms.	39
Fig. 11.	Durations of principal areas.	39
Fig. 12.	Maximum total duration at a point within 80-mile circle.	39
Fig. 13.	Maximum continuous duration at a point within 80-mile circle.	39
Fig. 14.	Spatial distributions of total water for some area storms.	54
Fig. 15.	Seasonal distribution of area storms.	56

Fig. 16.	Digital map of AN/CPS-9 intensity levels, 2130 EST, 9 July 62.	58
Fig. 17.	Distribution of maximum precipitation intensity at a point for band storms.	61
Fig. 18.	Distribution of maximum hourly intensity over 80-mile circle for band storms.	61
Fig. 19.	Examples of spatial intensity distributions in bands, 14 June 63 and 26 July 62.	62
Fig. 20.	Durations of entire storms.	66
Fig. 21.	Durations of single bands.	66
Fig. 22.	Maximum total duration at a point within 80-mile circle.	66
Fig. 23.	Maximum continuous duration at a point within 80-mile circle.	66
Fig. 24.	Histogram of hourly areal intensity, 6-8 Nov 59.	68
Fig. 25.	Distribution of band lengths.	72
Fig. 26.	Distribution of band widths.	72
Fig. 27.	Spatial distributions of total water for some band storms.	78
Fig. 28.	Film prints of AN/CPS-9 RHI echoes on 1510 EST, 16 Nov 60, and 1708 EST, 28 May 63.	81
Fig. 29.	Seasonal distribution of band storms.	81a
Fig. 30.	One-hour rain-gauge patterns for 0100 EST, 2 March 63 and 1100 EST, 9 July 62.	90
Fig. 31.	Seasonal distributions of storms in area, band and miscellaneous groups.	93

LIST OF TABLES

Table 1.	Total water amounts and intensities for area storms.	32
Table 2.	Durations within 80-mile circle for area storms.	38
Table 3.	Maximum durations at any point within 80-mile circle for area storms.	41
Table 4.	Dimensions of areas of various intensities for area storms.	43-45
Table 5.	Synoptic data, type of precipitation, and equivalent rainfall rate adjustment for area storms.	49
Table 6.	Spatial distributions of total water in area storms.	52
Table 7.	Total water amounts and intensities for band storms.	59
Table 8.	Areal durations, number of bands, and areal intensity histogram peaks for band storms.	64
Table 9.	Maximum durations at any point within 80-mile circle for band storms.	65
Table 10.	Band dimensions and orientation.	70-71
Table 11.	Synoptic data for band storms.	74
Table 12.	Spatial distribution of total water in band storms.	77
Table 13.	Characteristics of storms containing miscellaneous patterns.	84
Table 14.	Characteristics of storms containing precipitation areas, bands and miscellaneous patterns.	87

I INTRODUCTION

A detailed knowledge of the mesoscale precipitation patterns associated with larger-scale synoptic situations would be of considerable interest in the study of precipitation physics and small-scale atmospheric circulations. In addition, such knowledge would be of help in making local forecasts. The actual structure of mesoscale systems and the characteristics of the associated precipitation patterns are known only in the most general way. For example, it is recognized that summer disturbances are likely to produce convective storms which contain relatively high intensity precipitation over small areas, whereas winter disturbances more frequently produce stratiform-type storms which spread low-intensity precipitation over relatively large areas. On the other hand, little is known about such characteristics as the actual dimensions of the precipitation areas, the actual variation of intensities within them, or the total amounts of water deposited over areas of various sizes; nor is the relationship between these characteristics and the larger-scale parameters well understood.

There has been relatively little investigation of this question on a broad scale. Mesoscale observation networks have been inaugurated for limited areas of the country by the

National Severe Storms Project (Fujita, 1963), but the data from these networks are primarily thunderstorm data and do not cover other types of storms in a representative way. Also, such networks cover surface data only. Radar has the advantage of being able to scan in three dimensions over a range sufficiently large to be useful in mesoscale pattern studies and has been used extensively in qualitative investigations. However, only recently have there existed sufficient quantitative radar data to permit a quantitative study of mesoscale precipitation patterns.

Previous studies of mesoscale precipitation patterns have tended to concentrate on a few storms of a particular type. Swisher (1959) investigated rainfall patterns of five instability lines in New England by using a combination of radar data and reports from the U.S. Weather Bureau rain-gauge network. He found that such storms tend to intensify in the area of the Berkshires to the Connecticut River and dissipate as they move eastward toward the coast. This study was extended by Cochran (1961) who made a numerical study of nine squall lines with a moving grid. He found two modes of squall line development but no detectable difference between them in the associated synoptic conditions. Stem (1964) used a 10 cm radar in conjunction with synoptic data to study seven thunderstorm situations. He was primarily interested in the internal structure of individual thunderstorms but also included consideration of the mesoscale patterns and

their environment. In particular, his investigation pointed up the tendency of thunderstorm complexes to form or persist in areas of larger-scale convergence associated with frontal zones or sea breezes. Noel and Fleisher (1960) applied a screening and multiple regression technique to investigate the linear predictability of stratiform precipitation patterns as depicted on a radar scope. From a study of ten storms they found that predictors selected by the screening process gave a mean reduction of variance significantly larger than that obtained by either persistence or advection alone. However, this statistical study of predictability provided very little information on mesoscale precipitation patterns as such. Boucher and Wexler (1961) investigated the prediction from radar observations of behavior of precipitation lines, and Boucher (1961) later extended the study to precipitation areas. Both studies, in which AN/CPS-9 Plan Position Indicator (PPI) normal data were used, were concerned primarily with motion and duration and gave no information on intensities and internal structure of the echoes. Finally, Taylor (1962) made a study of storm water budgets to determine whether stratiform or convective storms were more efficient in precipitating out the available water. He used both radar and rain-gauge network data to determine the precipitation in a fixed volume of atmosphere through which the storms passed. Consideration of two convective and three stratiform storms indicated that the stratiform type was more efficient in precipitating the available water with about 17 per cent compared with 5-8 per cent for the convective type.

The purpose of this study is to find objective criteria by which mesoscale precipitation patterns in the eastern New England area can be recognized and characterized. The storms studied were first classified with respect to pattern on the radar scope and then, within the pattern class, were grouped according to their similarity with respect to such mesoscale characteristics as total amount of precipitation, the dimensions of precipitation patterns, the intensity distribution, and the duration of the precipitation in the area. They were also grouped according to larger-scale synoptic characteristics such as the type of front in the area, distance from and type of low center associated with the precipitation pattern, air mass disturbance, and immediate history of the storm. Each of the mesoscale groups is compared with the others and with the synoptic groups, and any interdependence of the mesoscale characteristics or dependence upon the larger-scale synoptic patterns is assessed.

The mesoscale characteristics were obtained from both radar and rain-gauge data. Both suffer certain limitations in defining the amount and distribution of precipitation over a given area, but the limitations of one cover different parameters from those of the other so that, in most cases, the radar and rain-gauge data tend to supplement each other.

II DATA AND METHODS OF ANALYSIS

A. Radar Measurements

Data

The radar data used in this investigation are in the form of integrated, range corrected, iso-echo contours observed with the AN/CPS-9 and SCR 615-B radars located at the Massachusetts Institute of Technology and operated by the M.I.T. Weather Radar Project. The pertinent basic radar parameters for each radar are listed below:

	<u>AN/CPS-9</u>	<u>SCR 615-B</u>
Wave length	3.2 cm	10.7 cm
Beam width (between one-half power points)	1°	3°
Pulse length	600 m (for long pulse)	450 m
Antenna gain	41.6 db	33 db
Transmitted power	250 kw	450 kw

The SCR 615-B is used primarily in summer convective storms since at its relatively long wavelength the radiation is not subject to attenuation by rain. The AN/CPS-9 is used primarily in winter stratiform situations where greater sensitivity

is needed and the possibility of attenuation is greatly reduced.

Kodaira (1959) has described the instrumentation for the iso-echo contours for which the signals are range-corrected and the audio frequency fluctuations are averaged out. These contours may be displayed directly on the PPI of either the SCR 615-B or AN/CPS-9 radars and photographed on 35 mm film. A cinematograph camera with an automatic stepping switch changes the intensity level every second scan of the antenna and provides a complete sequence of iso-echo contours every three or four minutes. There are approximately five db between the threshold values of intensity levels.

Interpretation of Radar Data

For range-corrected signals each intensity corresponds to a definite radar reflectivity per unit volume, denoted by η , which is defined as the sum of the back scattering cross-sections of all the particles in a unit volume of atmosphere. The radar equation in abbreviated form is:

$$\bar{P}_r r^2 = c \eta$$

where \bar{P}_r is average returned power, r is range, and c is a constant which depends on the radar parameters. From a careful measurement of the parameters of the AN/CPS-9 and SCR 615-B radars at M.I.T., Austin and Geotis (1960) have shown that values of η measured by these radars are accurate to 3 db or less.

The relationship of η to rainfall rate R is usually obtained through the use of the radar reflectivity factor, Z , which is defined as

$$Z \equiv \sum n_i d_i^6$$

where n_i is the number of particles of diameter d_i per volume. For non-spherical particles d_i represents the diameter of spheres of mass equal to that of the non-spherical particles. If the scatterers are small, Z and η are related by the expression

$$\eta = \frac{\pi^5}{\lambda^4} \left| \frac{\epsilon - 1}{\epsilon + 2} \right|^2 Z$$

where λ is the wave length of the radar radiation and ϵ is the complex dielectric constant of the scattering particles.

The parameter Z is not uniquely related to the precipitation rate, but a number of measurements of particle size distributions in natural precipitation have provided useful empirical relations, some of which have been summarized by Batten (1959). Marshall and Palmer (1948) suggested a relation of $Z = 200 R^{1.6}$ where R is in mm/hr, and where the scatter of measured points was about 3 db. This relationship was selected for the present study as being most representative for a large variety of storms. For the above relation, an interval of 5 db between threshold values of the intensity levels corresponds to a factor of two in rainfall rate between one value and the next. Also, the combined uncertainties in the measurement of η , deduction of Z , and application of the Z - R relation indicate that the limit of accuracy obtainable

in rainfall rate measurements by the AN/CPS-9 and SCR 615-B radars can be expected to be roughly a factor of two.

It should be mentioned here that the relation $Z = 200 R^{1.6}$ applies only to rain. A satisfactory expression for snow has not been found but Batten's summary indicates that the range is from $600 R^{1.8}$ to $2000 R^{2.0}$. For the sake of convenience, both rain storms and snow storms are treated in the same way with respect to reflectivity. If $Z = 200 R^{1.6}$ is used for rain, then

$$\eta = \frac{\pi^5}{24} \left| \frac{\epsilon-1}{\epsilon+2} \right|^2 \times 200 R^{1.6} = \text{constant} \times R^{1.6}$$

However, the factor $\left| \frac{\epsilon-1}{\epsilon+2} \right|^2$ is 0.93 for water but only 0.20 for ice. Therefore, if the same constant is used for dry snow as for rain, the following Z-R relation is implied:

$$Z \approx 1000 R^{1.6}$$

Thus, for convenience and ease of analysis the expression $Z = 200 R^{1.6}$ is used for rain and $Z = 1000 R^{1.6}$ is used for snow. As a check, a comparison of radar values of precipitation rate obtained from these relations with actual rain-gauge measurements is made for each storm.

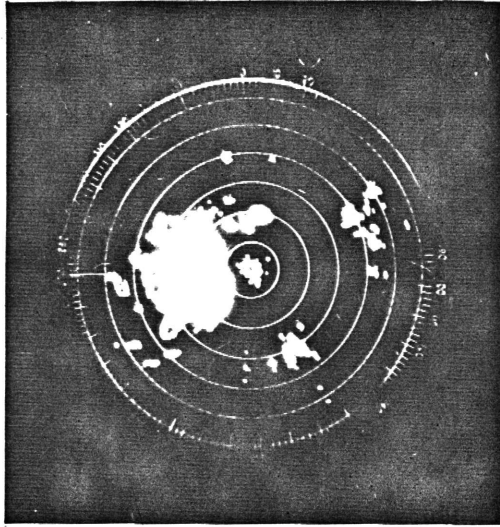
Because of uncertainties in the composition, size, and shape of the hydrometeors observed, radar observations cannot be considered as direct measurements of Z and R. Therefore, values of these quantities which are deduced from measured radar reflectivities are designated equivalent reflectivity factor and equivalent precipitation rates, denoted Z_e and R_e respectively.

Method of Analysis

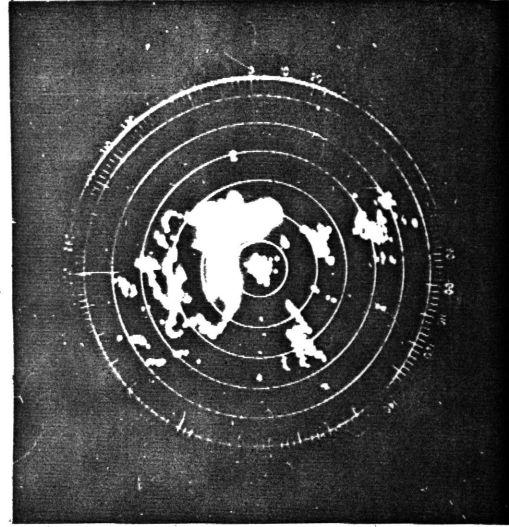
In order to obtain a quantitative representation of the intensity levels the filmed data were reduced at ten-minute intervals to digital maps which represent the display in terms of average intensity level in 5 x 5 mile squares. Fig. 1 shows for 0530, 20 March 63, the actual pictures of the AN/CPS-9 scope at various intensity levels from which the digital maps were obtained. Such a map is shown in Fig. 2. This was accomplished by projecting the scope photographs upon the grids and marking the appropriate intensity numbers in each square.

There is a certain amount of subjectivity in determining the average intensity level for small echoes, especially for those which straddle two grid squares, but this was reduced as much as possible by setting up rules for approximations. For instance, if a square is half filled or more at any level it is considered to be totally filled, but a square less than half filled is considered to be empty; if a small echo straddles two or more squares it is recorded in only one, and so forth. It is believed that random subjective tracing errors tend to cancel out.

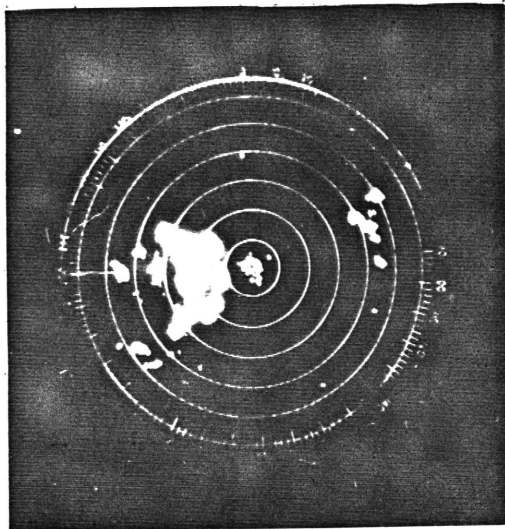
A receiver calibration was made at the time of each observation. The calibration data were plotted as a series of curves representing the minimum power returned for each



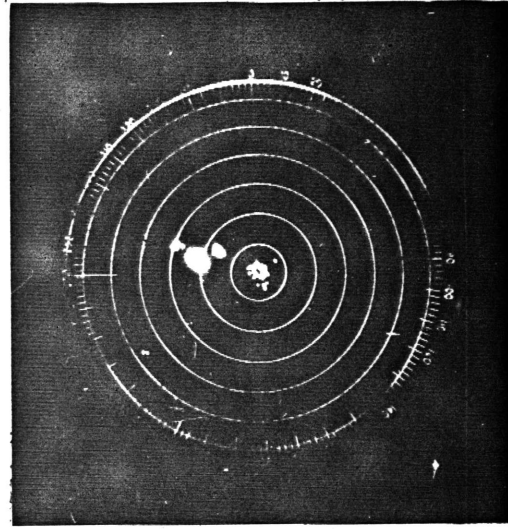
L-2



L-3



L-4



L-5

Fig. 1. Photographs of iso-echo contours on PPI, levels 2-5, taken at 0530 EST on 20 Mar 63. Range markers are at 20-mile intervals.

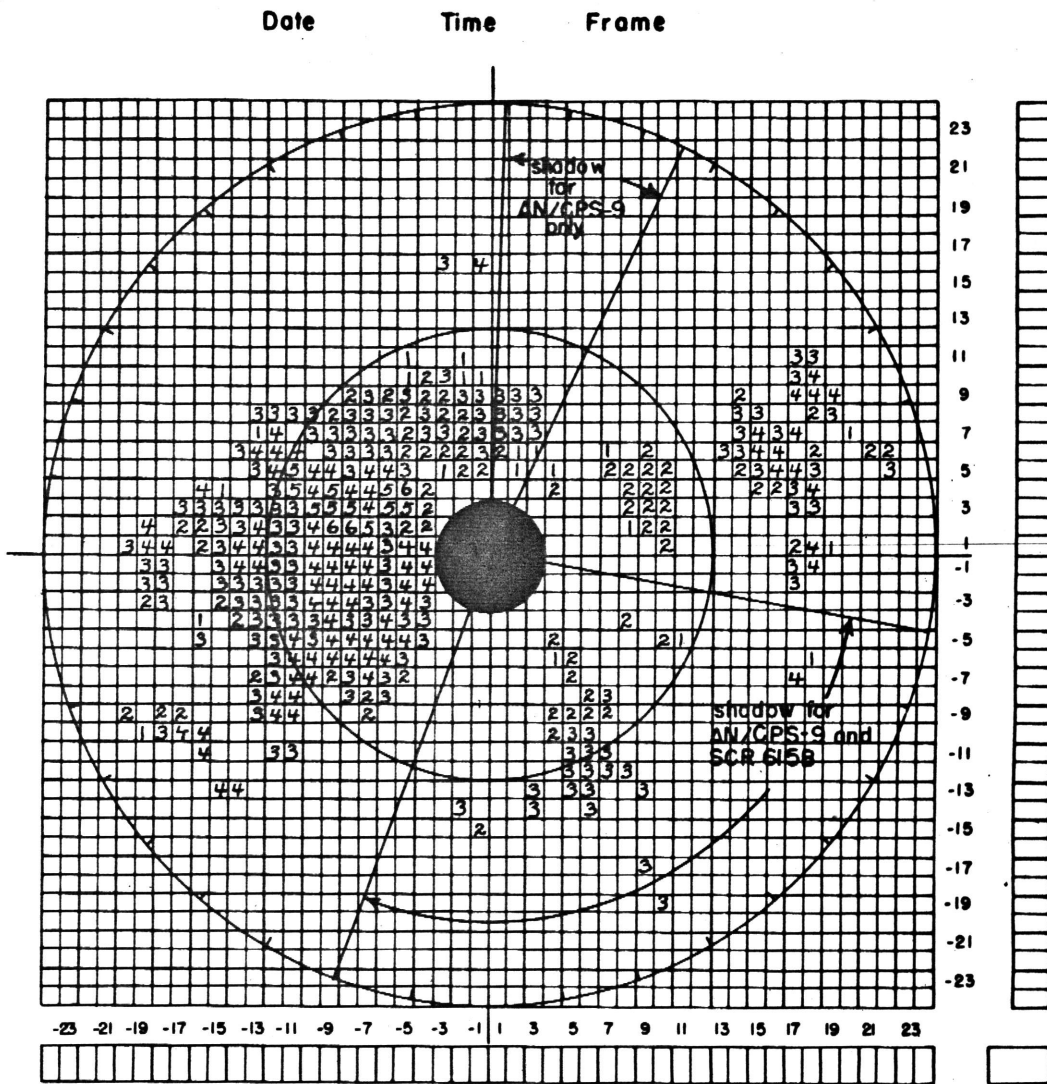


Fig. 2. Digital map of AN/CPS-9 intensity levels 1-6 at 0530 EST on 20 March 63. Range markers at 60 and 120 miles.

intensity level as a function of range. The graph was compared to a standard graph computed from the radar equation with equivalent rainfall rates based on the relation $Z = 200 R^{1.6}$ ($Z = 1000 R^{1.6}$ for snow). This procedure gives the corresponding equivalent rainfall rates of the successive intensity levels for each observation in terms of 0.25, 0.50, 1, 2, 4, 8 mm/hr by factors of two up to 500 mm/hr. These specific values were assigned so that one storm could be compared with another, but this procedure may have involved some errors if the thresholds were not at just the right place. Some of the values were rounded off for computational convenience. Fig. 3 shows the theoretical graph and a calibration graph taken from an actual observation. As can be seen in the actual calibration, the threshold values of the intensity levels are not always 5 db apart, thus requiring some of the levels to be combined in assigning equivalent rainfall rates. The equivalent rainfall rates were used to determine intensities and amounts of precipitation and to compare the radar data with the rain-gauge data.

The effective range of the radar depends upon the intensity and height of the precipitation and, thus, varies considerably from storm to storm. The actual range of the scope is 120 miles, but under the best conditions precipitation measurements with the two radars used in this study appear to be realistic to a range of no more than 80 miles. In some storms factors such as limitations of detectability or intrusion of the melting layer into the beam restrict the useful

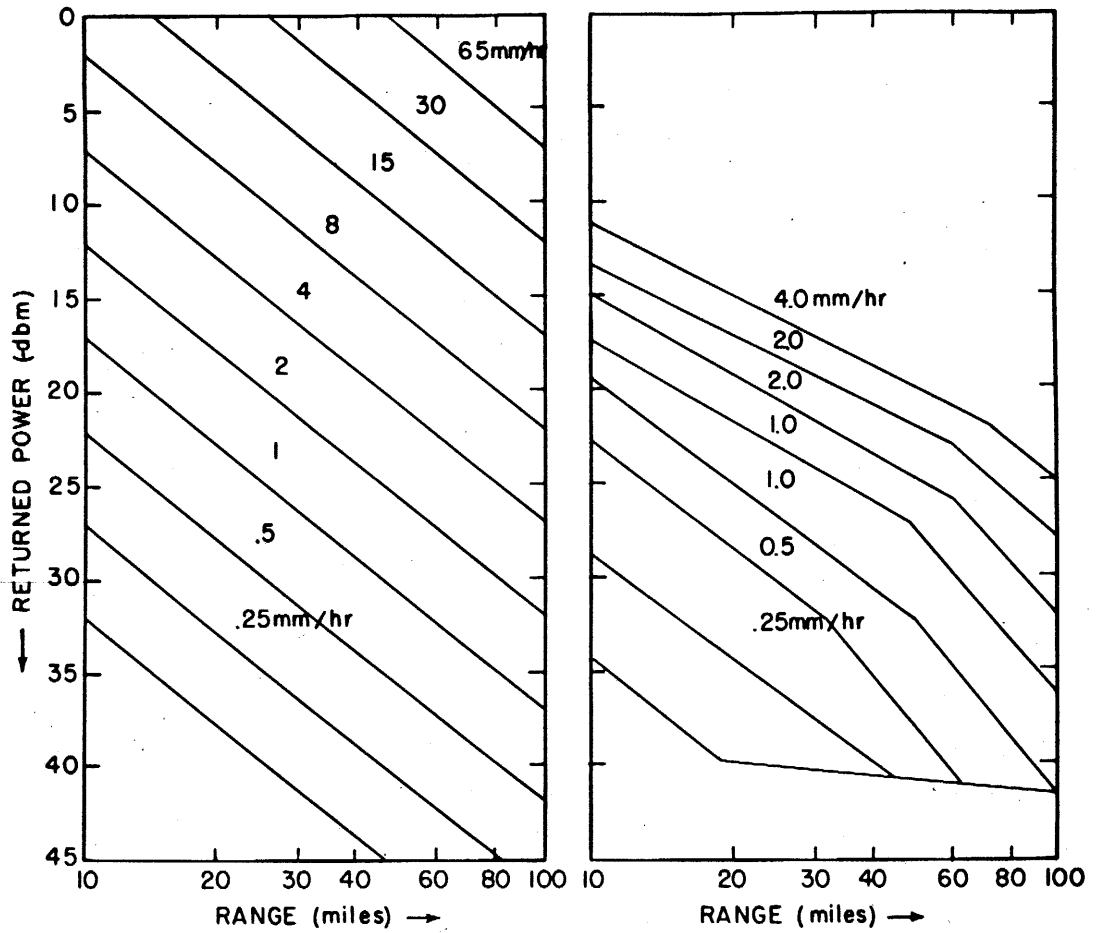


Fig. 3. Theoretical and actual (21 March 63) calibration curves for the AN/CPS-9 radar. Values of returned power in the calibrations reflect a 50 db cable loss.

range to only 30 or 40 miles. For the present study, a circle of radius 80 miles centered at Cambridge, Massachusetts was considered for the purpose of measuring the total water and a range of 120 miles for the qualitative definition of pattern, etc.

Because the radar is blocked by higher buildings in the southeast quadrant, data in a sector from 100° to 200° were excluded. Also, several thin smokestacks to the north seriously affect echoes on the AN/CPS-9 but not on the SCR 615-B which has a wider beam. Thus, for the AN/CPS-9 only, data in a sector from 360° to 23° were also excluded. The positions of these "shadow" areas are indicated in Fig. 2.

From the digital maps the following information was tabulated:

a. Pattern. The three types of pattern were designated area, band, and miscellaneous. In cases of band precipitation, both the number of bands and their orientation were noted. In cases of area type precipitation, the number and orientation of the areas, if they were elongated, were noted.

b. Dimensions. The dimensions of the principal precipitation areas were noted where possible. In most cases the maximum values of the dimensions during the observation were those recorded.

c. Maximum intensity at a point. The highest intensity of precipitation reached by the storm at a point within effective range of the radar was obtained; this was taken to be the highest equivalent rainfall rate found in any 5 x 5 mile square outside the shadow sectors. In some cases, especially in the area patterns, if the highest intensity appeared extremely isolated or possibly spurious, the next highest equivalent rainfall rate was taken as being more representative.

d. Intensity distribution. Histograms of intensity distribution corresponding to various times during the radar observation were made. These were obtained from the total number of squares in each intensity contour level for all the levels at the time of the digital map.

Limitations

It has already been noted in the Introduction that one advantage of the radar is that it is able to scan in three dimensions. The radar also has the advantage of complete coverage and high resolution in both time and space.

On the other hand, the radar suffers from some definite limitations. The relation $Z = 200 R^{1.6}$ is empirical and does not necessarily apply to all types of precipitation. There is considerable doubt about the validity of $Z = 200 R^{1.6}$ for some coastal storms off New England, especially those which occur in the fall as they appear to contain smaller drop sizes

than other types of storms in other seasons. In such cases, the radars see much less rain than do the rain gauges. Also, a Z-R relation for snow has not been satisfactorily established, and the assumed expression, $Z = 1000 R^{1.6}$, is more expedient than reliable.

Horizon and range effects also limit the radar data. The hills around the Boston area raise the horizon to about 0.5° and thus make it necessary to run the radars at a 1° elevation angle. As the range increases the volume sampled by the radar increases with size and is at a higher elevation as shown in Fig. 4. At 1° elevation the center of the radar beam at 60 miles is 7300 ft above the surface, at 80 miles is 10,500 ft, and at 120 miles is nearly 18,000 ft. This may mean that in many winter stratiform storms at medium ranges the beam is above the main precipitation. It also may mean that in some cases the radar may see precipitation aloft at higher levels that is not representative of what reaches the ground.

Attenuation represents a serious limitation to short wave length radars such as the AN/CPS-9. Gunn and East (1954) have shown that 3.2 cm radiation would suffer a 90 per cent power loss in each round trip mile traveled in 100 mm/hr rain, whereas 10 cm radiation would suffer only 2.3 per cent. Thus, radiation from the AN/CPS-9 can be easily attenuated, either by high intensity precipitation for short path lengths or by moderate intensity precipitation over long path lengths.

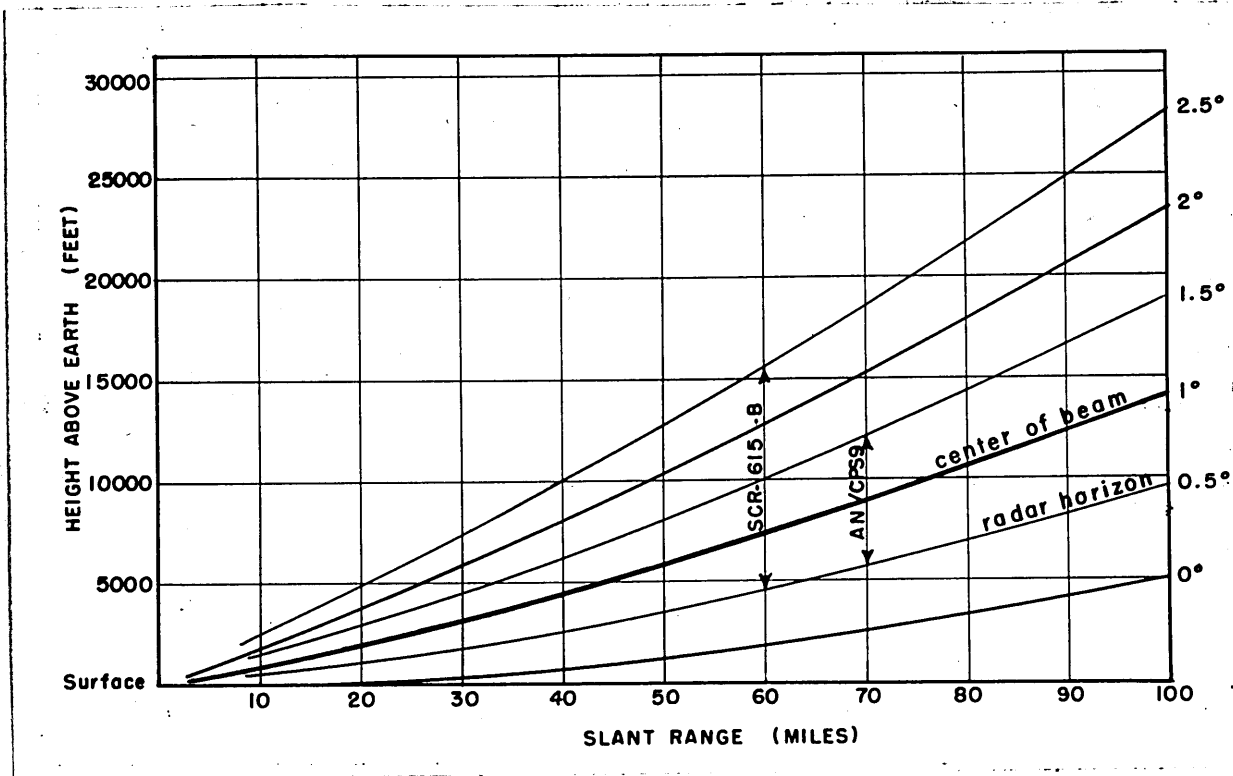


Fig. 4. Curves showing position and spread of radar beams at elevation angle of 1°. Radar horizon is at 0.5° because of low hills in vicinity.

Therefore, the AN/CPS-9 is used much more extensively during the winter when precipitation is relatively light and attenuation causes little difficulty. On the other hand, the SCR 615-B is generally used in the spring and summer when high intensities make attenuation of the AN/CPS-9 a much more serious problem.

While the SCR 615-B is not troubled by attenuation, it does lack resolution and sensitivity. The relatively wide beam causes uncertainties in deducing dimensions of the precipitation areas, especially at large ranges. The lack of sensitivity, on the other hand, causes light precipitation

to go undetected completely, and even moderate precipitation may be missed except at short ranges. The minimum detectable signal varies from one observation to another. In general, the SCR 615-B detects 8 mm/hr to about 60 miles, 4 mm/hr to about 40 miles, but rarely detects 2 mm/hr at any range.

Finally, there are some limitations in the time coverage by the radars. They were not always operating for the full duration of a storm, and there were occasional interruptions in the PPI display while Range Height Indicator (RHI) pictures or other measurements were being taken.

B. Rain-Gauge Data

Data

The rain-gauge data used in this study were obtained from a network of 69 gauges located in central and eastern New England within a range of 120 miles from Cambridge, Mass. The records from these gauges are summarized by hour, day and month in pamphlets published by the U.S. Weather Bureau. Fig. 5a shows the locations of these gauges. In order to have quantities comparable with those of the radar, the rain-gauge network used was limited to 80 miles (39 gauges) for quantitative measurements and 120 miles for qualitative considerations.

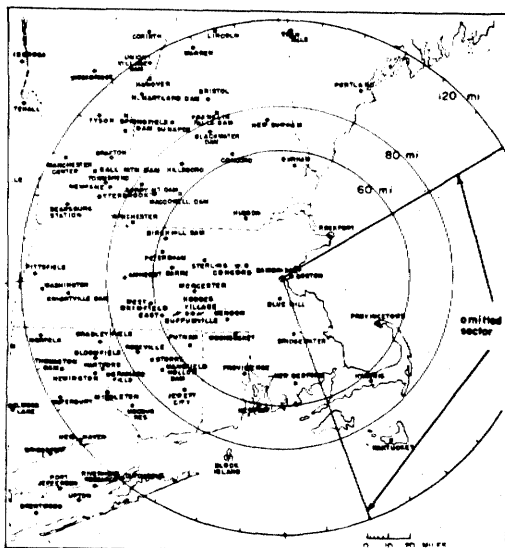
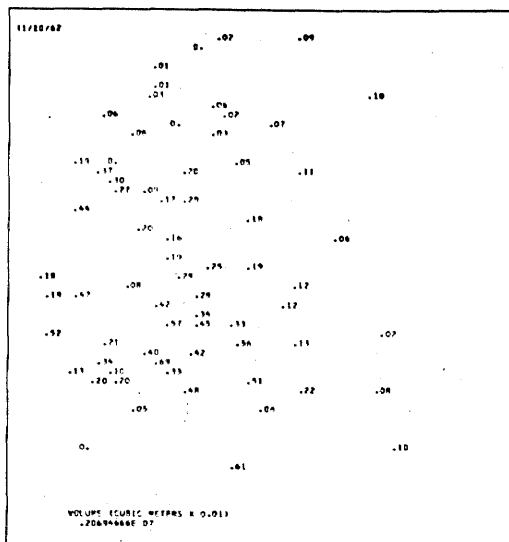
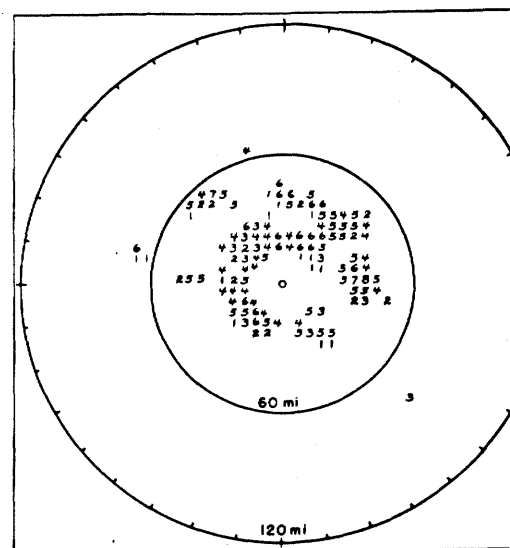


Fig. 5a. Map of rain gauge stations reporting hourly amounts in New England.



b. Example of computer output for 1000 EST, 10 Nov 62 showing hourly rainfall in inches and total water deposited within 80-mile circle.



c. Digital map of radar echoes on AN/CPS-9 at 0910 EST, 10 Nov 62.

Analysis

A computer program was written to plot data from the 120-mile network on hourly maps and to compute the total amount of water deposited within the 80-mile circle for the hour. Such a map, which includes the total water for the hour, is shown in Fig. 5b. Similarly, maps were plotted for 24-hour rain-gauge total amounts, and the 24-hour total water for the circle was computed. Since the gauge density varies, the hourly amounts of each gauge were weighted for the total water computation by the area the gauge best represents.

This area was determined by the use of irregular polygons formed from perpendicular bisectors of lines drawn from each station to adjacent stations. A sector of the circles from 60° to 160° was omitted because there are no rain gauges over the ocean. Fig. 5a shows the position of this sector. The size of the sector is the same as the southeast "shadow" used for the radar data, although not exactly in the same location. Thus, the areas defined for rain-gauge and radar computations are made comparable, though not identical (see Fig. 2).

From the rain-gauge hourly data the following information was tabulated:

- a. Pattern. In the cases of stratiform precipitation, the number of major areas and their orientation, if any, were noted.

b. Dimensions. The dimensions of the major precipitation bands and/or areas were recorded, where possible. Maximum values were used.

c. Total water. The total water deposited by the entire storm within the 80-mile circle was recorded. Also, a histogram of the hourly distribution of the total water was made. An example is shown in Fig. 6.

d. Maximum intensity over the entire 80-mile area. This was taken to be the highest peak of the areal intensity histogram in cubic meters of water per hour (see Fig. 6).

e. Maximum point duration of continuous precipitation. This was defined to be the maximum length of time any gauge received continuous measurable precipitation. It is used as a measure of the uniformity or continuity of the precipitation.

f. Maximum total duration of precipitation at a point. This quantity was defined as the maximum length of time from the start of measurable precipitation at any station to the final end of precipitation at that station. This may cover periods of time when no precipitation was recorded at the station.

g. Total duration of precipitation within the 80-mile area. This is the total duration that precipitation existed anywhere within the 80-mile area.

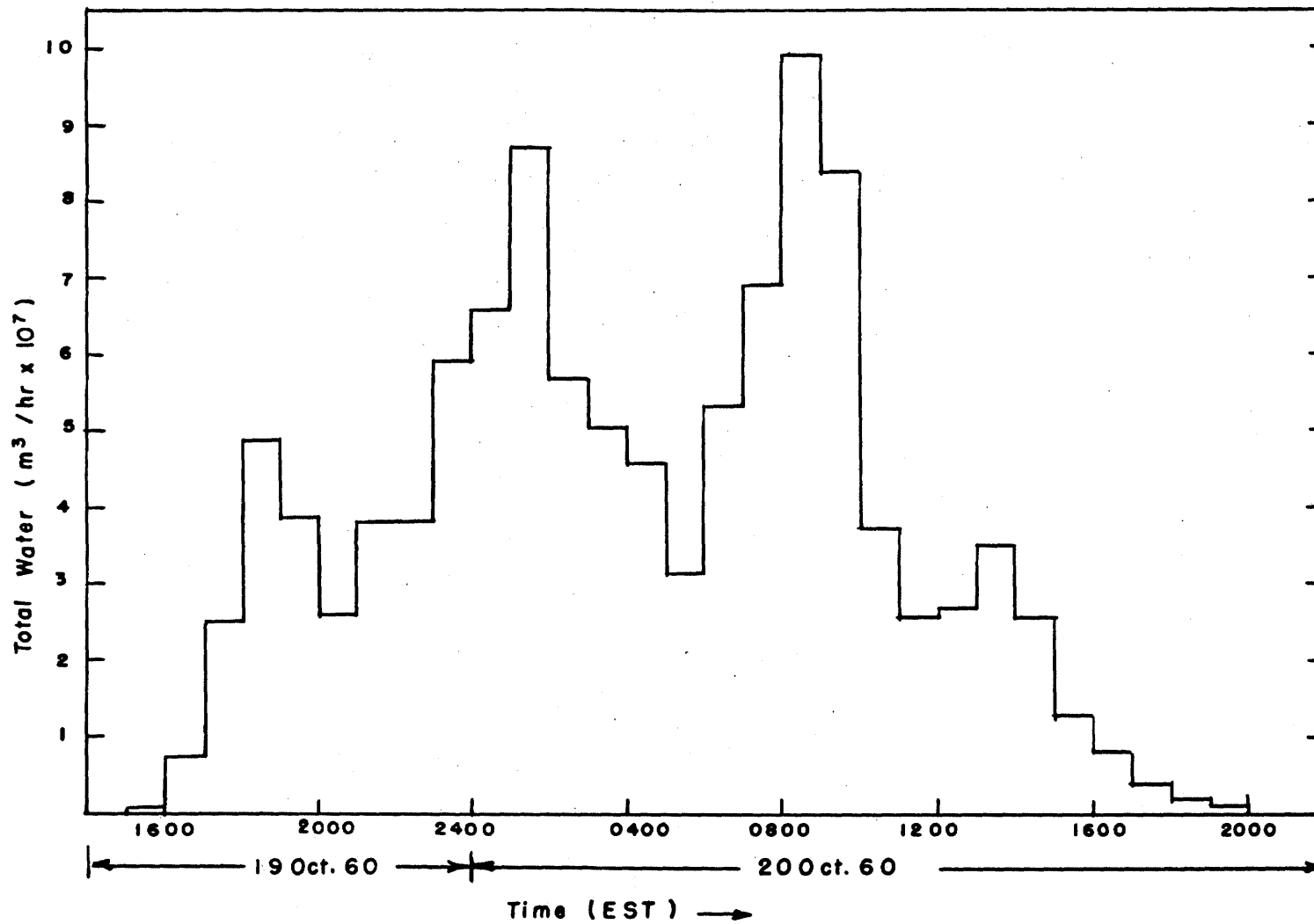


Fig. 6. Histogram of hourly areal intensity (total deposit within 80-mile circle) for 19-20 October 60.

Limitations and Approximations

The major limitation of the rain-gauge network is lack of sufficient coverage. This situation is aggravated by the wide variation in the spacing of the gauges. It is particularly unfortunate that so few stations are within a range of 30-40 miles of the radar (see Fig. 5a). As a result of the poor resolution and irregular gauge density, individual convective cells and even convective cell complexes can move between the gauges without hitting them in a representative way, and in some cases without hitting them at all. Since the area represented by each gauge is not equal to the area represented by other gauges, the gauges in less dense areas may make spuriously high contributions to the computed total water if one or more of them is hit by a small intense storm or cell. Here, the radar is valuable since it views continuously over the entire effective range.

Errors may also arise as a result of approximations made to facilitate the total water computation program. Sometimes, particularly during snow storms, one or more gauges reported a total precipitation amount for the entire storm or for a number of hours rather than hourly amounts. In these cases the total was divided evenly over the indicated (by an asterisk in the data) hours. At other times a dash was inserted for each hour a gauge received precipitation but neither hourly nor final totals were given. Here, where the dashed hours were consistent with the presence of precipitation in

the general area (as indicated from nearby stations) a value of .01 inch was inserted. Both of the latter procedures may result in distortions of the hourly distribution of total water as computed by the machine, but it is believed that the approximations are better than none at all.

C. Comparison and Combination of Radar and Rain-Gauge Data

Point and Area Comparisons

Both the radar and the rain-gauge data were used to check and to supplement each other because of the limitations and many possibilities for error when either set of data is used alone. First, the radar data for each observation were compared with the corresponding rain-gauge data point by point. Such a comparison indicates the extent to which the radar and rain gauges agree. If there was significant disagreement, the reason was sought. This procedure consisted of taking for each hour a representative sample of gauges and comparing the amount of precipitation reported by each gauge with the amount indicated by the radar for the 5 x 5 mile square in which the gauge was located.

When the point by point comparison indicated either general agreement (defined to be within a factor of two) or random disagreement with no tendency for either radar or rain gauges to read consistently high or low relative to the other,

the equivalent rainfall rates assigned from the calibration were considered reliable, and the total water and intensity distributions were computed. In those cases, where the radar consistently indicated either greater or lesser amounts than the rain gauges by at least a factor of two, the equivalent rainfall rates were adjusted to agree with the gauges. In such cases, the computation of total water was done solely from the rain-gauge data. It was assumed that either the Z-R relation which was used was not applicable or that the precipitation sampled by the radar was not representative of that reaching the surface, and that under these conditions, the radar could not adequately measure precipitation amounts.

The rain-gauge data served as a check upon the radar's effective range while the radar data provided information on intense areas that were smaller than could be resolved by the rain-gauge network. In general, it has been found that in stratiform situations where there is relative uniformity of precipitation in the horizontal, but where there is rapid variation in reflectivity with height, the rain gauges give more reliable data since the radar is often severely limited in range. Figs. 5b and 5c show a comparison of a digital map and the associated rain-gauge hourly map for 0900-1000 on 10 November 62. The effective range of the radar is only 50-60 miles whereas the gauges indicate precipitation much beyond but yet within the radar's mechanical range. On the other hand, in convective situations where the horizontal dimensions are relatively small and vertical uniformity is

relatively large, the radar data are more reliable than the rain-gauge data since the rain-gauge network lacks sufficient resolution.

While it may be recognized that band patterns are most often associated with summer convective situations and area patterns with winter stratiform situations, use of these relations in an exclusive manner is to be avoided. It is recognized that many stratiform storms have convective elements within them and that many area patterns represent precipitation that is convective in part. In a similar fashion, many band patterns may be composed of or include stratiform elements. Further research in the details of such relationships is needed but is beyond the scope of the present investigation.

Summary of Characteristics to be Obtained from Radar and Rain-Gauge Data

Listed below is a summary of those characteristics to be obtained from the radar data, rain-gauge data, and from a combination of both:

Radar only

- 1) Maximum intensity at any point 5 x 5 mile square within the effective range.
- 2) Intensity distributions during the observation.

Rain-gauge only

- 1) Maximum intensity over the 80-mile circle with the deleted segment.
- 2) Maximum duration of continuous precipitation in the area.
- 3) Maximum total duration of precipitation at a point (gauge).
- 4) Duration of precipitation anywhere within the 80-mile circle.

Radar and rain-gauge combined

- 1) Dimensions of precipitation areas.
- 2) General intensity of precipitation areas.
- 3) Time distribution of total precipitation intensity during the storm.
- 4) Total water for entire storm within a range of 80 miles.
- 5) Any information on the validity of the Z-R relation used in this study.

It might be added here that sometimes one kind of data (radar or rain-gauge) may be better suited than the other for the determination of one or more of the first four characteristics under the radar-rain gauge combination.

D. Synoptic Data

Data

The regularly transmitted facsimile and teletype data were used to study the large-scale synoptic features associated with each mesoscale precipitation pattern.

Emphasis was placed upon surface facsimile data with 500 mb data used as a supplement. Gaps in the surface facsimile data were filled in by hourly teletype data and U.S. Weather Bureau daily surface maps. The hourly data were sometimes used to obtain temperature and precipitation conditions during winter storms.

Analysis

The storms were grouped, according to their synoptic features, as frontal (cold, warm, occluded, and stationary fronts), air mass disturbances, overland low pressure centers and coastal low pressure centers. These features were assumed to be the cause of the precipitation in question. The recent history of each disturbance was noted, as well as the distance of the low pressure center, when appropriate, from the radar. The synoptic groupings were then compared to those obtained from the radar and rain-gauge data to discover what relation, if any, exists between them.

Limitations

It must be borne in mind that the temporal and spatial resolution of the synoptic data is, on the whole, quite poor. The surface facsimile and U.S. Weather Bureau daily maps were available for 12 hourly intervals only, as were the 500 mb charts. The poor spatial resolution is inherent in maps of large scale and may cause uncertainties

in the precise location of the features in question. When mesoscale systems are involved this may become important.

E. Data Selection

Since the purpose of this study is to seek relationships between the mesoscale patterns and precipitation amounts on the one hand and the macroscale characteristics on the other, storms for this study were chosen on the basis of pattern displayed by the radar. It was necessary to select those situations where the radar showed a fairly good coverage out to 60-80 miles. Such a criterion is inherently subjective and was applied with varying degrees of rigor to different types of patterns. Thus, patterns selected as areas were required to be moderately continuous during at least part of the observation, whereas band type patterns were required to be fairly continuous within the band pattern and to move through the 60-mile range area for a considerable distance during the time of observation.

Of the radar data available in digital maps, 71 cases met the above conditions and were divided into four groups by pattern: 1) bands or lines - 24 cases; 2) fairly widespread and continuous areas centered more or less over the radar during the major portion of the observation time (representing predominantly stratiform type patterns) - 28 cases; 3) moderate size continuous areas not centered on the radar for all or most of the observation time - 10 cases;

and 4) miscellaneous cases that appeared either to be a combination of the other pattern types or not to fit any of them at all - 12 cases. The latter two categories contain relatively few storms and represent less well-defined patterns than the first two. Hence, the bulk of this study is concerned with the first two groups and involves 52 cases of mesoscale precipitation almost equally divided between bands or lines and areas as seen on the radar scope. Some investigation of the miscellaneous group was made for comparative purposes.

III AREAS

A. Intensity and Amount of Precipitation

The results of the computations for the area patterns (see Fig. 2 for a typical radar area pattern) are summarized in Tables 1-6. In all of the tables the storms are listed in descending order of total water to indicate more easily the relation, if any, between total water and the other variables. Table 1 indicates the total water, maximum intensity at a point (maximum point intensity) and maximum total areal intensity for each storm. As defined in this study, the total water is the amount deposited during the entire storm within a range of 80 miles from Cambridge. Actually, a sector of 100 degrees is omitted from this circular area. For results based upon rain-gauge measurements the sector is due east over the ocean. For radar measurements the omitted sector is the southeast quadrant. Total area with the 100-degree sector omitted is approximately $4 \times 10^{10} \text{ m}^2$. Table 1 indicates that the values of total water range over an order of magnitude, from $11.8 \times 10^8 \text{ m}^3$, or a depth of about 30 mm, to $1.5 \times 10^8 \text{ m}^3$, or a depth of about 4 mm. As the storms are listed in the table there appears to be a fairly even distribution from highest to lowest values.

TABLE 1.
TOTAL WATER AMOUNTS AND INTENSITIES FOR AREA STORMS

<u>Date</u>	<u>Total Water (m³x10⁸)</u>	<u>Maximum Point Intensity (mm/hr)</u>		<u>Maximum Total Area Intensity (m³/hr x10⁷)</u>		
		4-8	15-30	0-6.9	7.0-13.9	>13.9
12-13 Mar 62	11.8	8			8.6	
10-11 Nov 62	11.6		30			23.9
19-20 Oct 60	11.0		30		9.9	
6 Mar 63	10.8	8				15.6
23-25 Oct 60	10.7		30		12.8	
19-20 Feb 63	9.7	4			10.8	
12 Feb 63	9.1	8			7.9	
21 Dec 60	9.1		30		12.4	
8-9 Mar 61	8.4	8			9.6	
18 May 63	7.6	4			10.8	
2-3 Feb 63	6.7	8			7.1	
11-12 Dec 60	6.4	8		6.2		
10-11 May 63	6.1		30		11.1	
1-2 Mar 63	6.1	8		5.7		
19 Feb 62	5.3	4			7.2	
10 Nov 60	5.0		15		7.1	
26 Feb 62	4.9	8		5.9		
20-21 Mar 63	4.5	4		2.5		
19-20 Jan 61	4.1	4		3.6		
15-16 Jan 61	3.4		15	3.0		
12 Mar 63	3.2	4		3.5		
22-23 Feb 61	3.1	8		5.7		
11 Jan 63	3.0	8			7.8	
13 Mar 63	2.1		15	5.1		
17-18 Apr 63	1.7	4		3.4		
14 Jul 61	1.7	8		3.1		
11 Jun 63	1.6	4		2.9		
3-4 Jun 63	1.5		30	3.0		

The maximum point intensity is the highest equivalent rainfall rate found in any 5 x 5 mile square outside the radar shadow areas. It represents an instantaneous rate and was based upon radar data since the gauges give only hourly amounts and also lack spatial coverage. The intensities range from 4 to 30 mm/hr with from 4 to 8 mm/hr being heavily favored (19 out of 28 cases). It is good to remember that since the values of the assigned equivalent rainfall rates differ by a factor of two, there is a fairly large margin of error for each value. Fig. 7 shows the distribution of the storms over the range of intensity and also the seasonal distribution for each intensity. The indication is that the late winter storms produce lower maximum point intensities (4-8 mm/hr) than storms at other times of the year. This may be due at least in part to the fact that the late winter storms tend to be snow storms which are usually lighter in intensity than rain storms because there is less available moisture in cold air. See Fig. 15 for a seasonal distribution of the 28 area patterns.

Whereas the maximum point intensity represents an instantaneous precipitation rate at a point, the maximum areal intensity is the maximum amount of water deposited over the 80-mile area within one hour and is taken to be the highest value on the areal intensity histogram of each storm (see Fig. 6). This intensity is based upon the rain-gauge data because the effective range of the radar was, in many cases, less than 80 miles. Table 1 indicates that the range

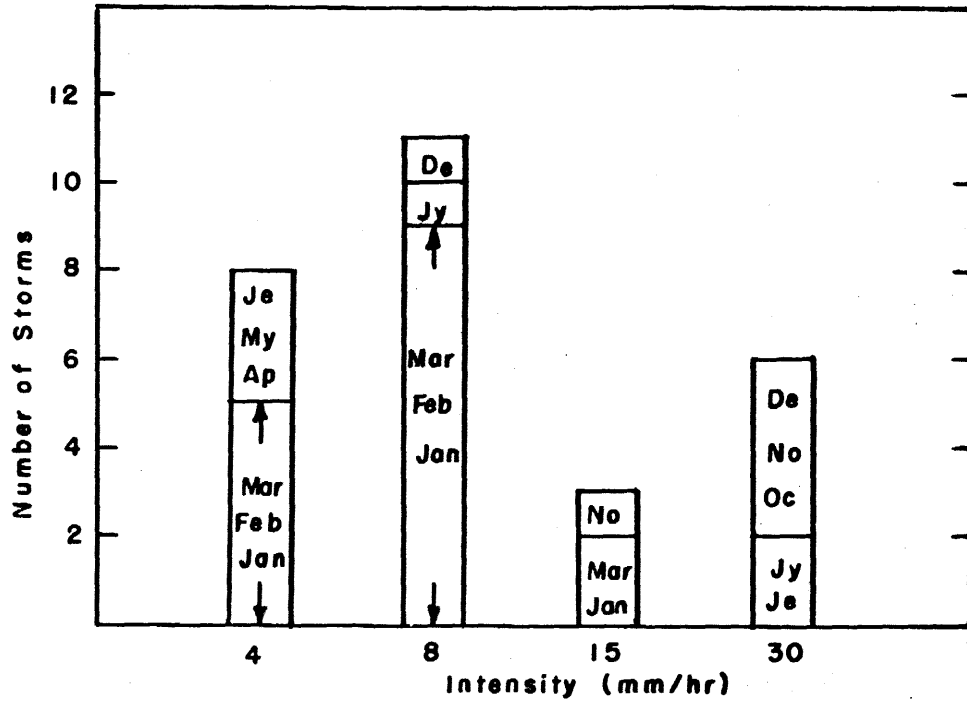


Fig. 7. Distribution of maximum precipitation intensity at a point showing seasonal distribution.

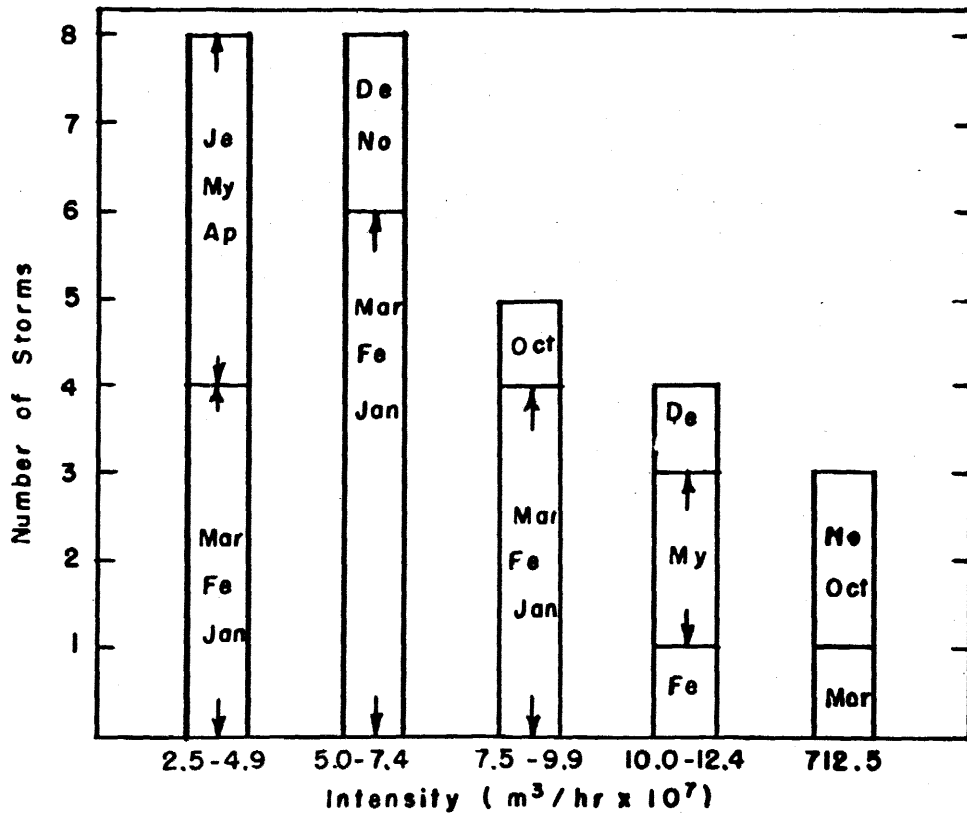


Fig. 8. Distribution of maximum hourly intensity over 80-mile circle showing seasonal distribution.

of maximum areal intensity is quite large but that most of the storms fall between 3×10^7 and $12 \times 10^7 \text{ m}^3/\text{hr}$ which corresponds to a depth of 0.7 to 3 mm over the whole area. The case of 10-11 November 62 appears to be unusual in that an extensive area of very heavy rain moved through central New England over a period of four hours causing an extremely high value of total water for those hours.

The seasonal distribution of the storms with respect to maximum areal intensity generally follows that of the maximum point intensity but somewhat less sharply, as shown in Fig. 8. Of the 21 storms with lowest areal intensity, 14 were storms in January through March.

From Table 1 there appears to be some relation between total water and maximum areal intensity but very little relation between total water and maximum point intensity. The higher intensities cover relatively small areas and apparently do not represent a major contribution to the total water. Fig. 9 shows distributions of intensity as shown on the AN/CPS-9 radar at various times during observations on 1-2 March 63. Only the area within the radar's effective range (with the shadow areas omitted) is represented in the histograms and thus may be only a small part of the total area of the 80-mile circle. The effective range on 1-2 March 63 was about 70 miles. The range of intensity is small, and fairly uniform precipitation is indicated by the areal predominance of one or two intensity levels.

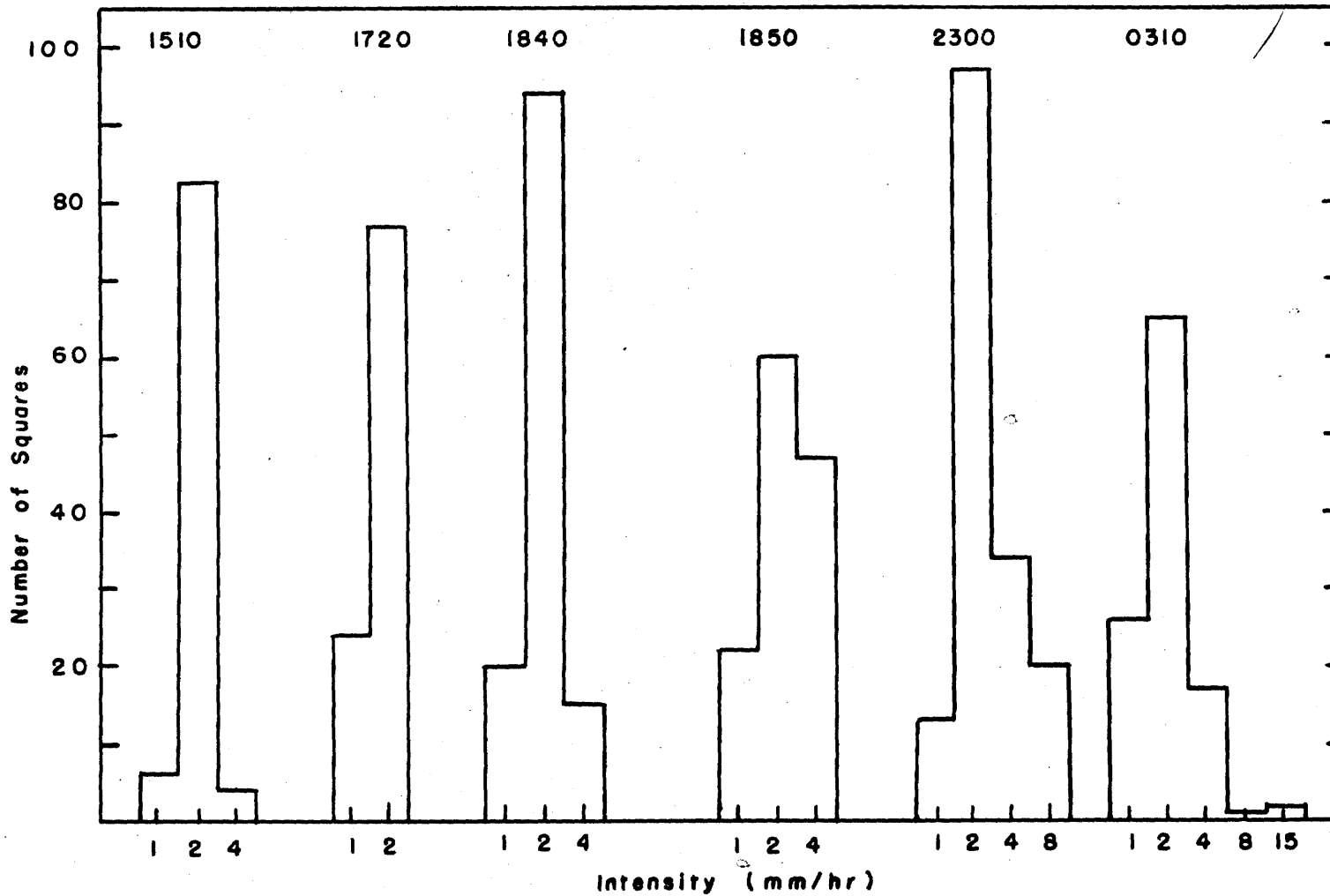


Fig. 9. Examples of spatial intensity distributions at selected times on 1-2 March 63.

B. Duration

Tables 2 and 3 summarize the results calculated for the characteristics relating to the duration of each storm. The duration characteristics described below were computed from the rain-gauge data alone because the radar's range was limited. Table 2 shows the total areal duration for each storm which is the total time that precipitation existed anywhere within the 80-mile circle. This includes hourly precipitation amounts of 0.3 mm or greater. The storms are spread out over quite a large range of total areal duration, varying from 8 to 48 hours. Fig. 10 represents the distribution over this range and indicates a peak at 16-19 hours. However, such a peak represents only 25 per cent of the storms considered, and a larger sample is needed to determine whether it is significant.

One cause of such a wide range in the total areal duration appeared to be the fact that some storms consisted of a major precipitation area preceded or followed by small areas or spots, usually of intensity less than 1 mm/hr, that persisted for some time. Such persistence of very light precipitation added to the total areal duration in a way that may not be really representative of the storm. The principal areal duration, defined to be the length of time that precipitation of at least 1 mm/hr existed within the 80-mile circle, was considered to be a more reliable estimate of the true length of the storm. The results are shown in Table 2, and the distribution is shown in Fig. 11. Most of the storms fall into a range of 8-27 hours with the peak again falling at 16-19

TABLE 2.

DURATIONS WITHIN 80-MILE CIRCLE FOR AREA STORMS

<u>Date</u>	<u>Total Area Duration (hours)</u>			<u>Principal Area Duration (hours)</u>			<u>No. of Areas & Bands</u>
	8-15	16-27	>27	8-15	16-27	>27	
12-13 Mar 62		26			26		1
10-11 Nov 62			35			28	2
19-20 Oct 60			29		27		3
6 Mar 63		16		12			2
23-25 Oct 60			48			46	3
19-20 Feb 63		18		15			-
12 Feb 63			31		23		2
21 Dec 60		23			20		1
8-9 Mar 61		23			22		1
18 May 63		22			17		1
2-3 Feb 63		22			19		1
11-12 Dec 60			34		19		1
10-11 May 63		26			17		3
1-2 Mar 63		21			17		1
19 Feb 62		17			16		1
10 Nov 60		27		12			1
26 Feb 62		18			16		1
20-21 Mar 63			34			34	1
19-20 Jan 61		27			27		1
15-16 Jan 61			30		25		2
12 Mar 63		19		15			1
22-23 Feb 61			30		23		2
11 Jan 63	13			9			1
13 Mar 63		16		9			2
17-18 Apr 63		17		13			2
14 Jul 61	15			9			several
11 Jun 63	14			10			several
3-4 Jun 63	8			8			1

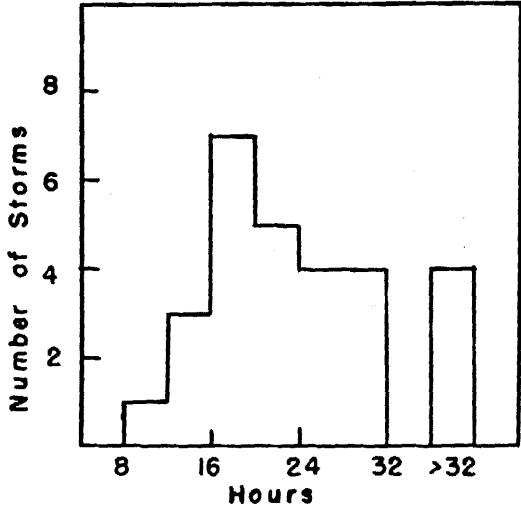


Fig. 10. Durations of entire storms.

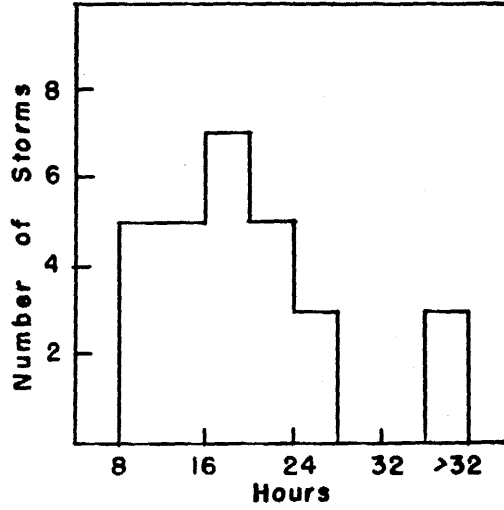


Fig. 11. Durations of principal areas.

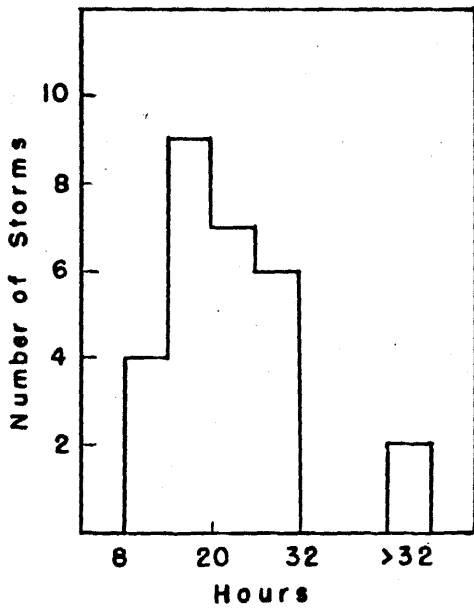


Fig. 12. Maximum total duration at a point within 80-mile circle.

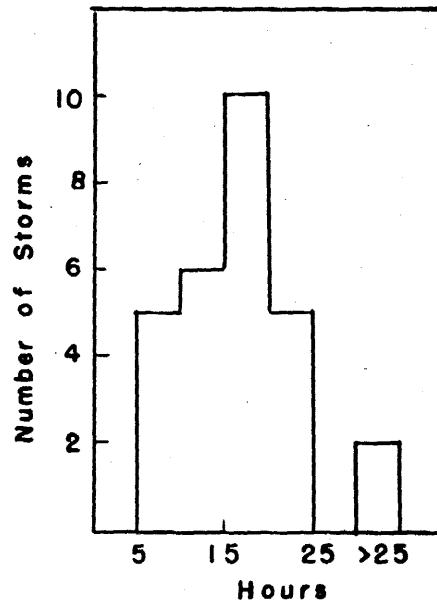


Fig. 13. Maximum continuous duration at a point within 80-mile circle.

hours. In those cases where there were two or more successive areas separated by one or more hours of precipitation less than 1 mm/hr, the principal areal duration was calculated from the beginning of the first area to the end of the last (see Table 2 for a list of the number of areas and bands for each storm).

Of some interest is the total length of time precipitation may persist at a single point within the area. The maximum total duration at a point (maximum point total duration) is defined as the maximum overall length of time over which measurable precipitation (0.3 mm/hr) existed at a rain gauge within the 80-mile circle. This quantity may include gaps in time when no precipitation was recorded by the gauge and is bounded only by the time of first and last recording of the gauge for the entire storm. However, the maximum continuous duration at a point (maximum point continuous duration) cannot include gaps in the record but represents the maximum length of time measurable precipitation persisted continuously at a gauge within the 80-mile circle. Table 3 shows the maximum point total duration and the maximum point continuous duration for each storm, and Figs. 12 and 13 indicate the distribution of storms with respect to these two characteristics. The peak appears at about the same place in both, 14-19 hours, whereas the range of the former is somewhat greater. The fact that the peaks fall over the same interval may be somewhat fortuitous since only six storms are common to both.

TABLE 3.
MAXIMUM DURATIONS AT ANY POINT WITHIN 80-MILE CIRCLE
FOR AREA STORMS

<u>Date</u>	<u>Maximum Point Total Duration (hours)</u>			<u>Maximum Point Continuous Duration (hours)</u>		
	8-15	16-24	24	5-9	10-19	20-30
12-13 Mar 62		21				20
10-11 Nov 62			31		12	
19-20 Oct 60			26			20
6 Mar 63	14				12	
23-25 Oct 60			47		17	
19-20 Feb 63		16			16	
12 Feb 63			27			23
21 Dec 60		22			18	
8-9 Mar 61		18			18	
18 May 63		22			15	
2-3 Feb 63		19			18	
11-12 Dec 60			28			22
10-11 May 63			25		12	
1-2 Mar 63		18			17	
19 Feb 62		16			15	
10 Nov 60		21			17	
26 Feb 62		17			13	
20-21 Mar 63			34			25
19-20 Jan 61		23				21
15-16 Jan 61			30			30
12 Mar 63		17			15	
22-23 Feb 61		23			12	
11 Jan 63	12			7		
13 Mar 63	13			8		
17-18 Apr 63	14			6		
14 Jul 61	11			8		
11 Jun 63	14				11	
3-4 Jun 63	8			8		

C. Dimensions

Table 4 summarizes the dimensions found for areas of various intensities. The sizes of the areas were evaluated on the basis of being at least 200, 100, 50, 30, or less than 30 miles in diameter. For those areas that were significantly elongated, two dimensions and the direction of the major axis are given. A general orientation for the whole area is given where possible in the columns to the right. For areas of 8 mm/hr or more, the dimensions as seen by the radar are also noted.

It is apparent that areas containing precipitation of 1-2 mm/hr were too large to be adequately defined by either the radar or the rain-gauge network but that the areas of 4 mm/hr and higher were usually small enough so that fairly reliable dimensions could be obtained by use of the radar and rain-gauge network. Specifically, in 20 out of 28 storms the 1 mm/hr area could not be defined, and in half of the storms the 2 mm/hr area could not be defined. On the other hand, only five storms contained areas of 4 mm/hr that could not be defined in all directions. With the exception of those areas on the border of the general region of consideration (120-mile radius centered at Cambridge) all areas of 8 mm/hr or greater could be well defined by the rain-gauge network.

All of the 28 storms contained areas of at least 4 mm/hr and most contained 8 mm/hr; half contained areas of 15 mm/hr and only five had areas of 30 mm/hr. Whereas the 1 mm/hr areas

TABLE 4.
DIMENSIONS* OF AREAS OF VARIOUS INTENSITIES
FOR AREA STORMS

<u>Date</u>	<u>Intensity (mm/hr)</u>					
	1	2	4	8	15	30
12-13 Dec 62	200	200	50 (30)	30 (30)		
10-11 Nov 62	200	200	200 (50)	100 (50)	50 (30)	
19-20 Oct 60	200	200x50/	50x30/	50x30/ (30)	(30)	(30)
6 Mar 63	200	200	200x100/ (50)	50x30/ (30)	(30)	
23-25 Oct 60	200x100	200x100	100x50 (100)	50x30 (50)	(30)	(30)
19-20 Feb 63	200	200	200x100-	200x100-		
12 Feb 63	200	200x100/	200x30/	(30)		
21 Dec 60	200	200	100	30 (30)	(30)	(30)
8-9 Mar 61	200	200	100x30/	30 (30)	30	
18 May 63	200	200x50	100x50/	50	(30)	(30)
2-3 Feb 63	200	100x50/	50x30-	30		
11-12 Dec 60	200	100	50x30/	(30)		

* Top value is from rain-gauge data. Line to right of each value indicates orientation of elongated areas with north at top of page. Values in parentheses are from radar data. Values of 200 are to be interpreted as "at least 200" and values of 30 as "30 or less".

TABLE 4. (Continued)

<u>Date</u>	<u>Intensity (mm/hr)</u>					
	1	2	4	8	15	30
10-11 May 63	200x100/	200x50/	200x50/	50x30/ (50)	50x30/ (30)	
1-2 Mar 63	200	100	50x30—	(30)		
19 Feb 62	200	200x100—	30 (30)			
10 Nov 60	200x100/	100x50/	50x30/	(100x30)/	(50x30)/	
26 Feb 62	200	100	50	(30)		
20-21 Mar 63	100	30 (30)	(30)			
19-20 Jan 61	200	100	30 (30)			
15-16 Jan 61	100x50	100	30	30 (30)	(30)	(30)
12 Mar 63	100x50	50	30 (30)			
22-23 Feb 61	200x50—	200x50—	30 (30)	(30)		
11 Jan 63	200x100	200x100	50 (50)	(30)		
13 Mar 63	100x50/	50	30	30 (30)	(30)	
17-18 Apr 63	100	50	50 (30)			
14 Jul 61		50	30 (30)	30 (30)	30	

* Top value is from rain-gauge data. Line to right of each value indicates orientation of elongated areas with north at top of page. Values in parentheses are from radar data. Values of 200 are to be interpreted as "at least 200" and values of 30 as "30 or less".

TABLE 4. (Continued)

<u>Date</u>	<u>Intensity (mm/hr)</u>					
	1	2	4	8	15	30
11 Jun 63	100x50—	50x30—	30			
				(100x30)—	(30)	
3-4 Jun 63	50	50	30 (30)	30 (30)		

* Top value is from rain-gauge data. Line to right of each value indicates orientation of elongated areas with north at top of page. Values in parentheses are from radar data. Values of 200 are to be interpreted as "at least 200" and values of 30 as "30 or less".

usually exceeded 200 miles in diameter, the 2 mm/hr areas varied widely from greater than 200 miles down to 50 miles in diameter. Most of the areas of 4 mm/hr and greater were on the order of 30 to 50 miles across, although a few of the 4 mm/hr areas were considerably larger.

In general, the radar was able to detect small areas of 15 and 30 mm/hr which were not detected by the rain-gauge network with its cruder space and time resolution. The small intense areas either moved between the gauges or moved across them fast enough so that the gauges did not receive the high intensity precipitation for an entire hour. There was general agreement between the radar and the rain-gauge network on the size of the 8 mm/hr areas.

Many of the areas were significantly elongated, having one dimension at least approximately twice the other or greater. The lines to the right of each column in Table 4 indicate the orientation of each area, where applicable, with north at the top of the page. The line indicates the orientation of an area of a particular intensity rather than the overall orientation. Twelve storms showed no overall orientation, although in four of them an area of a particular intensity showed some tendency in a specific direction. Of the 16 storms that showed some overall orientation, eight were in a northeast-southwest direction, four were east-west, and four were directed either north-south or northwest-southeast.

Of some interest are bands of more intense (4-8 mm/hr) precipitation embedded in an area of lighter (1-2 mm/hr) precipitation as seen by the radar. Four such cases were noted (12 December 60, 10 November 60, 20 January 61, 16 January 61). All of the bands were oriented northeast-southwest and were located within 50 miles of the radar. None of them were detected by the rain-gauge network, primarily because they were located in regions where the gauges are sparse. The duration of the bands varied from one to 12 hours. The dimensions, according to the radar, were about 60-100 miles in length and 20-30 miles in width (for the 4 mm/hr area).

Three storms had fairly well defined bands that were not embedded in lighter precipitation but were separate areas in themselves. These bands were greater than 200 miles in length and were 50-100 miles in width. Two cases, 19-20 October 60 and 23-25 October 60, contained three definable bands that moved through the area successively. The third case, 10-11 May 63 had a small area followed in succession by a fairly intense band and a very light band.

There appears to be little relation between the season of the storm and the size or shape of its definable precipitation areas.

The storms in this study were selected and grouped on the basis of their containing fairly obvious areas or bands of precipitation. It is apparent from the foregoing discussion, however, that a general system for classifying patterns must

include objective methods for defining areas, bands, and spots, and categories which include combinations of the three.

D. Cause of Precipitation

The results of this study indicate that the most frequent cause of area-type precipitation in the New England area appears to be coastal lows, the centers of which pass within about 150 miles to the south or southeast of the Boston area. Table 5 summarizes the synoptic data. Over half of the storms studied were associated with coastal lows, although five occurred in conjunction with systems that moved into the New England area from the west or southwest. The distance of the coastal low pressure centers from the Boston area at their nearest point ranged from zero to 180 miles with 10 centers passing within 100 miles. In some cases most of the precipitation over New England was received before the low pressure center reached its nearest point.

Other causes of area precipitation were warm fronts (7), occluded fronts (4), stationary fronts (3), low pressure systems from the west or southwest (5), and one semi-tropical storm. The warm fronts were associated with low centers that, in four cases, passed directly over New England and, in the other three cases, ranged in distance from 60 to 460 miles to the north and west. It is sometimes rather difficult to distinguish between a warm front and an occluded front as the causes of precipitation if the point at which the two fronts

TABLE 5.
SYNOPTIC DATA, TYPE OF PRECIPITATION,
AND EQUIVALENT RAINFALL RATE ADJUSTMENT FOR AREA STORMS

Date	Precip. Cause					Distance ⁺ : Low Center- Cambridge (miles)			Type of Precip.		Re [#] Adj.
	WF	DF	SF	CL	O*	0-100	101-200	>200	Rain	Snow	
12-13 Mar 62				x	x	70 S			x		4
10-11 Nov 62		x				60 N			x		
19-20 Oct 60	x					60 NW			x		
6 Mar 63				x		0				x	1/2
23-25 Oct 60	x					0			x		
19-20 Feb 63				x		90 SE				x	2
12 Feb 63				x		50 S				x	2
21 Dec 60	x						120 N		x		
8-9 Mar 61				x	x	50 S				x	2
18 May 63				x			170 S		x		
2-3 Feb 63		x					160 N			x	2
11-12 Dec 60				x			170 SE			x	
10-11 May 63				x	x		120 S		x		
1-2 Mar 63				x		70 S				x	8
19 Feb 62				x		80 S				x	
10 Nov 60		x						320 NW	x		
26 Feb 62				x			180 SE			x	2
20-21 Mar 63				x	x			240 SE		x	1/2
19-20 Jan 61				x			140 E			x	1/2
15-16 Jan 61				x	x		150 SE			x	
12 Mar 63				x		100 SE				x	2
22-23 Feb 61			x	x		80 S			x		
11 Jan 63			x					460 SW	x		
13 Mar 63	x				x	0				x	
17-18 Apr 63	x	x				0			x		
14 Jul 61	x		x					460 W	x		
11 Jun 63	x					0			x		
3-4 Jun 63					x			320 SW	x		

* "Other" includes overland low pressure centers from the Great Lakes or further south.

Values are the factor by which the radar equivalent rainfall rates were multiplied to bring them into general agreement with the rain-gauge data.

+ Distances and directions are for low center at its closest point to Cambridge.

merge passes over New England. Distinctions were made, except in the case of 17-18 April 63, but may be regarded as somewhat doubtful. Of the three stationary fronts, two were oriented east-west and tended to move north and south back and forth across New England, whereas the third was oriented northwest-southeast and remained well to the southwest of New England. The storm of 3-4 June 63 was altogether different from the rest and appeared to be of tropical origin.

Some investigation was made of the synoptic features of the longer storms to determine whether there were any particular features which tended to be associated with exceptionally long storms (arbitrarily defined as 30 hours or more in total duration). No definite conclusions were obtained since the sample of storms (28) was quite small. Some interesting tendencies were found, however, although these features were also exhibited to some degree by shorter storms. Most of the longer storms (see Table 2) had closed lows at the 500 mb level associated with the surface low centers, and when the upper air low moved slowly over New England, the surface low center also moved slowly. In addition, the close association of the surface low center with a low center aloft caused many of the long storms to intensify rapidly as they approached New England either as a coastal low or an overland low. With the rapid intensification the circulation of the storm increased in scope, and precipitation often extended northward into Canada, southward along the coast as far as North Carolina, and, in some cases, westward as far as the Great Lakes.

Finally, a third condition that appeared to contribute to the length of the storms was the presence of more than one synoptic system. The most frequent situation was that of the merging over New England of a coastal low and a low center from the west or southwest. Such a situation again tended to spread precipitation over a wider area than in those situations where only one system was involved. A much larger sample is needed to ascertain the real significance of these features in the determination of a storm's duration over New England.

E. Spatial Distribution of Total Water

The results of an analysis of the rain-gauge maps of the total amount of water deposited at each gauge for the entire storm within a distance of 120 miles from Cambridge are summarized in Table 6. The ratio of the highest to the lowest values found anywhere within the area is computed for each storm, where possible, to give an indication of the spread of the depth over the area. The cause of the precipitation as well as the total water over the whole area are included for the sake of comparison.

It was found that there was considerable variation in the pattern of the spatial distribution of the total water. The patterns of the coastal lows fell very broadly into two groups: those that exhibited the largest depth of water in the southern or southeastern part of the area (10) and those

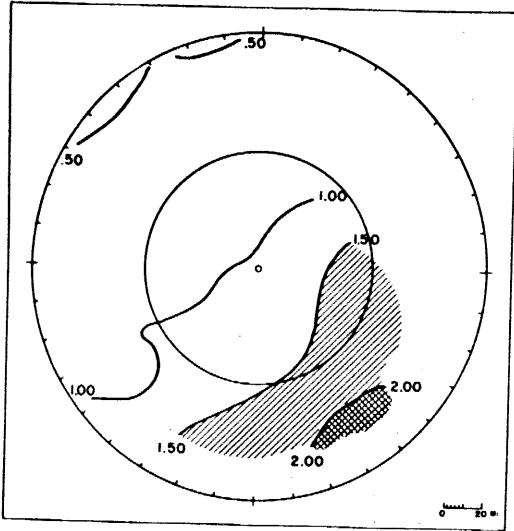
TABLE 6.

SPATIAL DISTRIBUTIONS OF TOTAL WATER IN AREA STORMS

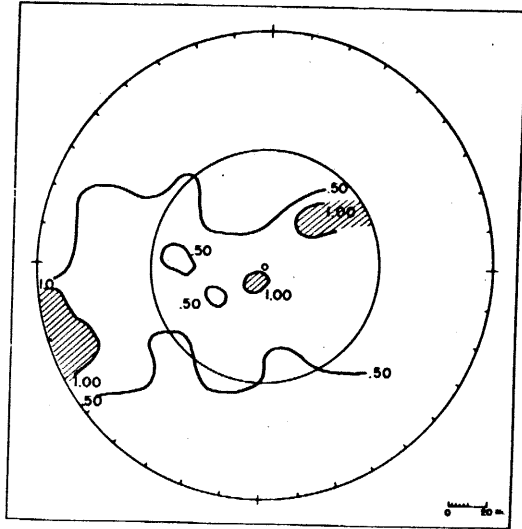
<u>Date</u>	<u>Location of Heaviest Precip. Center</u>			<u>Precip. Cause</u>	<u>Highest Amount (in.)</u>	<u>Lowest Amount (in.)</u>	<u>Ratio</u>
	<u>SW-SE</u>	<u>Band</u>	<u>Other</u>				
12-13 Mar 62	x			CL	2.37	.55	4.3
10-11 Nov 62	x			OF	2.55	.44	5.8
19-20 Oct 60	x			WF	2.02	.53	3.8
6 Mar 63	x			CL	1.83	.42	4.4
23-25 Oct 60			x	WF	1.99	.35	5.7
19-20 Feb 63	x			CL	1.61	.30	5.4
12 Feb 63	x			CL	2.04	.40	5.1
21 Dec 60	x			land low	1.71	.51	3.4
8-9 Mar 61		x		CL	2.33	.26	9.0
18 May 63	x			CL	1.39	.17	8.2
2-3 Feb 63			x	OF	1.07	.23	4.7
11-12 Dec 60	x			CL	2.08	.22	9.4
10-11 May 63		x		CL	1.14	.15	7.6
1-2 Mar 63	x			CL	1.16	.24	4.8
19 Feb 62		x		CL	1.07	.12	8.9
10 Nov 60		x		OF	1.42	.07	20.3
26 Feb 62	x			CL	1.10	.15	7.3
20-21 Mar 63		x		CL	.93	.12	7.7
19-20 Jan 61	x			CL	1.65	.17	9.7
15-16 Jan 61		x		CL	1.20	.12	10.0
12 Mar 63		x		CL	.81	.13	6.2
22-23 Feb 61	x			CL	.92	.06	15.6
11-12 Jan 63			x	SF	1.06	.34	3.1
13 Mar 63		x		land low	.60	.07	8.7
17-18 Apr 63	x			WF, OF	.42	.04	10.5
14 Jul 61			x	WF, SF	.96	.00	--
11 Jun 63			x	WF	.94	.00	--
3-4 Jun 63			x	tropical	.61	.00	--

that showed some evidence of a band oriented generally east-west across the middle of the area (6). Many of the storms in both groups also exhibited areas or spots of greater depth in other parts of the 120-mile circle, such as to the north or northwest, but these appeared in more of a random manner and were not considered to be the dominant feature. It is possible that the areas of heavier precipitation in the south also represent bands which cannot be defined by the rain-gauge network because they are on the edge of the network. Similarly, some of the areas of greater precipitation far to the north may represent bands of which the rain-gauge network can see only part. The storms in the second group did exhibit broken or spotty bands that were more or less definable by the network, and these appeared to be about 100 miles in width and, in most cases, at least 200 miles in length. Fig. 14 shows the patterns for storms in both groups.

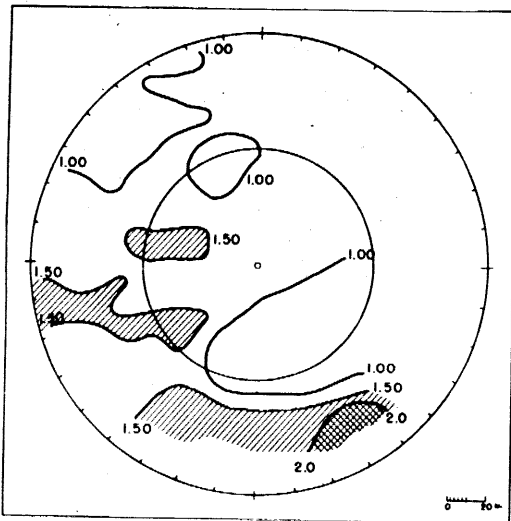
The remaining 12 storms, consisting of warm, occluded, and stationary fronts, showed patterns that were not greatly different from those of the coastal lows but which showed somewhat less organization. There was no particular pattern that could be definitely associated with any frontal type of activity, and since there was some difficulty in distinguishing between precipitation caused by a warm front and that caused by the associated occluded front or stationary front, all of the "frontal" storms were included in one group. The one storm of tropical origin was rather arbitrarily included in this group.



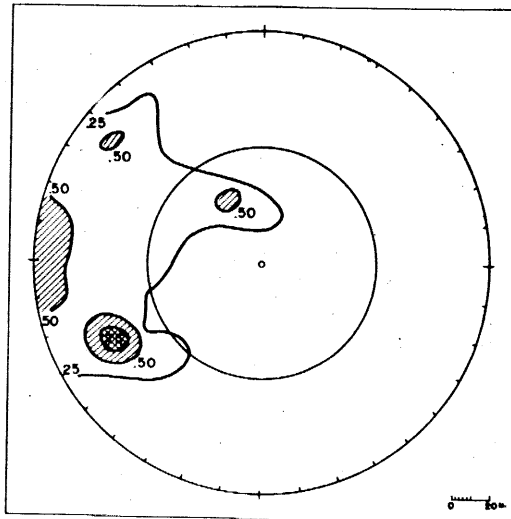
Coastal low
12 February 63



Coastal low
15-16 January 61



Warm front
19-20 October 60



Tropical storm
11 June 63

Fig. 14. Spatial distributions of total water for some area storms.

In nearly all of the storms precipitation appeared over the entire 80-mile area. Three storms had at least one gauge that received no precipitation, but only the storm of 3-4 June 63 (of tropical origin) had extensive areas where no precipitation was received (see Fig. 14). Table 6 shows the highest and lowest amounts of water received by the gauges within the 80-mile area. The ratio of these two values represents the uniformity of the precipitation over the area. Lower values of this ratio are, in general, associated with the storms of higher total water, indicating that the more uniform the storm is, the greater will be the total amount of water it deposits.

F. Seasonal Distribution

The seasonal distribution of the area type storms, as shown in Fig. 15, is quite uneven. By far the greatest number of storms selected occurred in January through March, and most of these were snow storms. Why is there such a disproportionate number of storms in January through March? Is it because they are snow storms or because more coastal storms occur at this time of year? Austin (1964) has reported several instances where radar reflectivity in fall New England coastal storms was exceptionally low as a result of small drop sizes. It is entirely possible that more fall coastal storms were not chosen for this study because the radar reflectivity was low and the scope pattern was poor, whereas

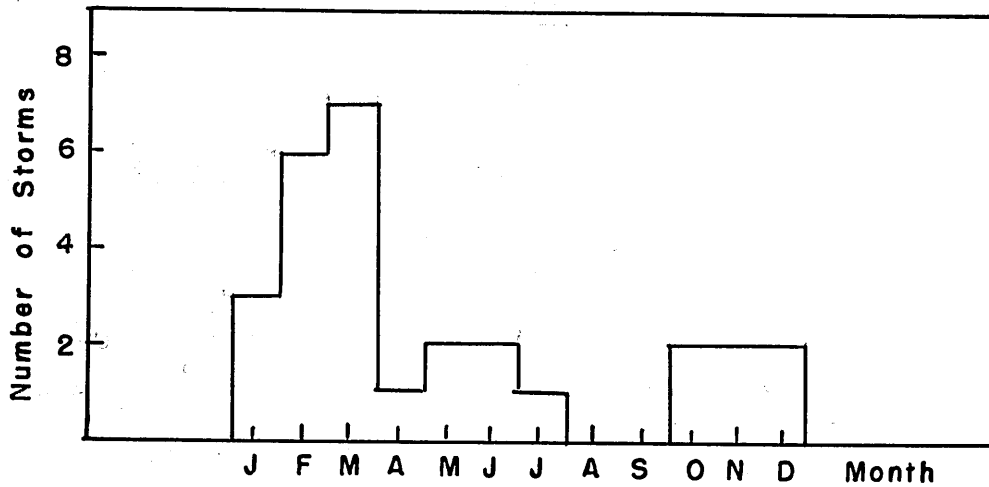


Fig. 15. Seasonal distribution of area storms.

in the late winter season this characteristic was not so prominent. Again rain storms do tend to be less uniform in intensity than snow storms; hence, the latter may have given more uniform radar patterns and thus stood a better chance of being chosen for this study. Also, heavy rain storms were often viewed on the SCR 615-B rather than on the AN/CPS-9 with the result that the pattern may have appeared quite spotty because of the low sensitivity of the SCR 615-B.

A wider investigation on properties of mesoscale precipitation patterns is currently under way. It includes almost all storms for a period of three years which deposited significant amounts of precipitation in the area, rather than just a few storms selected on the basis of radar coverage. In this study, bias which results from radar performance will be largely eliminated.

IV BANDS

A. Intensity and Amount of Precipitation

The results of the computations and analysis of the band patterns (see Fig. 16 for a typical radar band pattern) are summarized in Tables 7-12. As in the case of the areas, the storms are listed in order of descending values of total water in order to facilitate the comparison of total water with the other variables. The last two storms in each table are special cases and will be discussed separately.

The values of total water range over more than an order of magnitude, from $16.5 \times 10^8 \text{ m}^3$, or a depth of about 40 mm, down to $0.4 \times 10^8 \text{ m}^3$, or a depth of about 1 mm. The storms are rather unevenly distributed over this range with over half of the 22 values falling between 10^8 and $4 \times 10^8 \text{ m}^3$. From Table 7 it is evident that for the bands the range of maximum point intensity is quite large and that the maximum point intensity of most of the storms is quite high. Fig. 17 shows the distribution. Values of 65-130 mm/hr are the most common, but the entire range is from 8 to 250 mm/hr. Geotis (1963) has found that a reflectivity corresponding to an equivalent rainfall rate of 100 mm/hr or greater is usually indicative of hail.

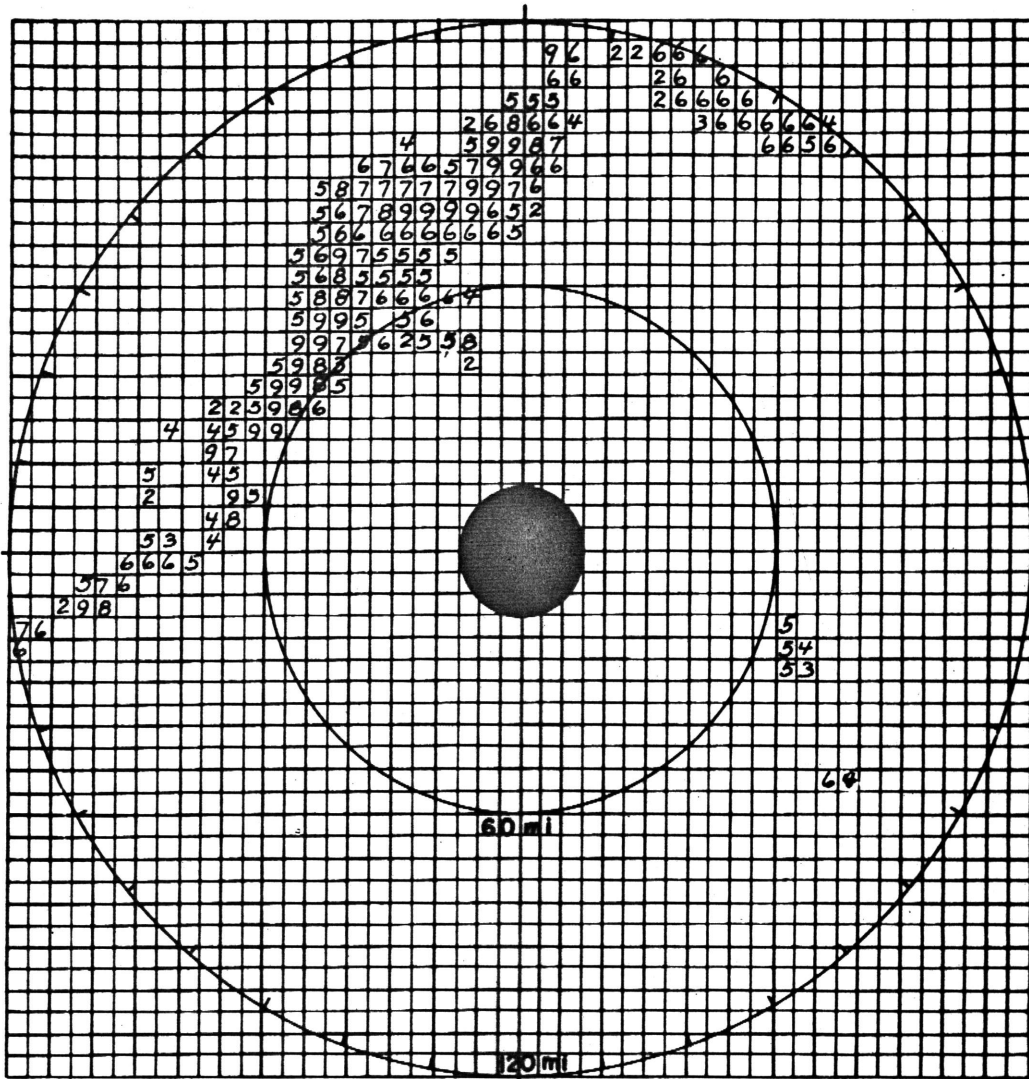


Fig. 16. Digital map of intensity levels 2-9 on AN/CPS-9 showing band pattern at 2130 EST on 9 July 62.

TABLE 7.

TOTAL WATER AMOUNTS AND INTENSITIES FOR BAND STORMS

<u>Date</u>	<u>Total Water (m³x10⁸)</u>	<u>Maximum Point Intensity (mm/hr)</u>		<u>Maximum Areal Intensity (m³/hr x10⁷)</u>		
		4-30	65-250	0-4.9	5-9.9	>9.9
26-28 May 61	16.5		130		9.5	
30 Oct-1 Nov 62	15.9	15			7.4	
8 Jul 63	9.5	30			9.3	
6-8 Nov 59	8.8	15			5.0	
9 Jul 62	7.6		130			17.2
17 Aug 62	5.9		65		8.5	
2 Jul 61	4.5		130			14.6
2-4 May 62	3.5	15		2.1		
31 May 62	3.2		250		8.0	
24 Jun 60	2.6		130		6.9	
26 Jun 62	2.3		250		8.6	
14 May 63	2.0		65		5.4	
23 Oct 62	1.9	15		3.6		
7 Aug 63	1.9		65			10.0
26 Jul 62	1.9		130	4.4		
20 May 63	1.8		65		7.0	
9-10 Oct 62	1.5	8		1.1		
29-30 Jun 60	1.5		130	2.1		
21 Jul 62	1.2		130	4.1		
1 Aug 63	.8	30		3.0		
14 Jun 63	.7		65	2.3		
21 Jul 63	.4	8		1.1		
16 Nov 60	(2.0)	(15)				
28 May 63	(1.2)	(4)				

The low value at 30 mm/hr may be caused by instrumental bias. It is possible that more storms with maximum point intensities in the 30 mm/hr range were not chosen for this study because they show rather spotty patterns on the relatively insensitive SCR 615-B. The SCR 615-B was operated during storms of this intensity in order to avoid attenuation, but at the same time it missed much of the lighter precipitation which, on the AN/CPS-9, would have provided a better pattern. The range of the maximum areal intensity is rather small, and the values are fairly evenly distributed as shown in Fig. 18. It is somewhat bimodal in nature with peaks between 2×10^7 and $6 \times 10^7 \text{ m}^3$ and between 8×10^7 and 10^8 m^3 , but these may be insignificant in such a small sample. From Table 7 it may be seen that the maximum areal intensity exhibits some positive relation to the total water.

The intensity of precipitation within the bands varied over a wide range. Fig. 19 shows the spatial intensity distributions at selected times during radar observations on 14 June 63 and 26 July 62. The areal coverage of these storms is quite small as indicated by the number of squares for each intensity. In both cases the radar was able to detect the bands at least 80 miles away.

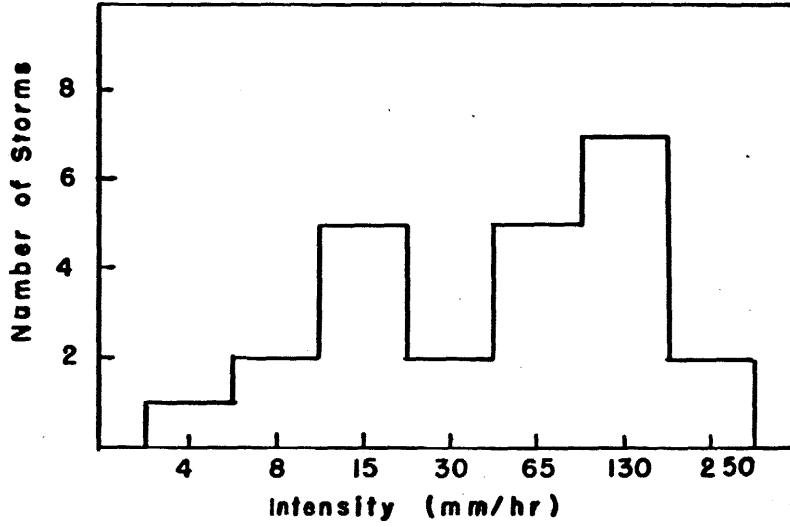


Fig. 17. Distribution of maximum precipitation intensity at a point for band storms. Includes the special cases.

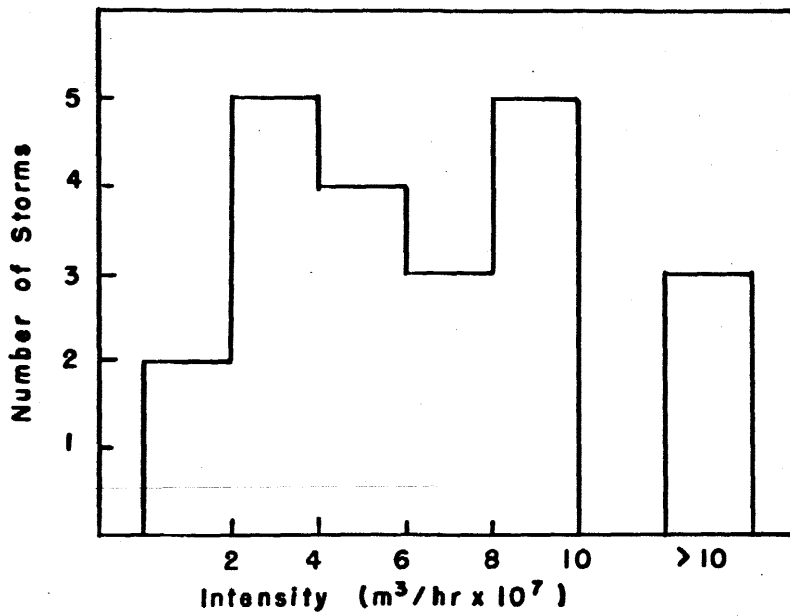
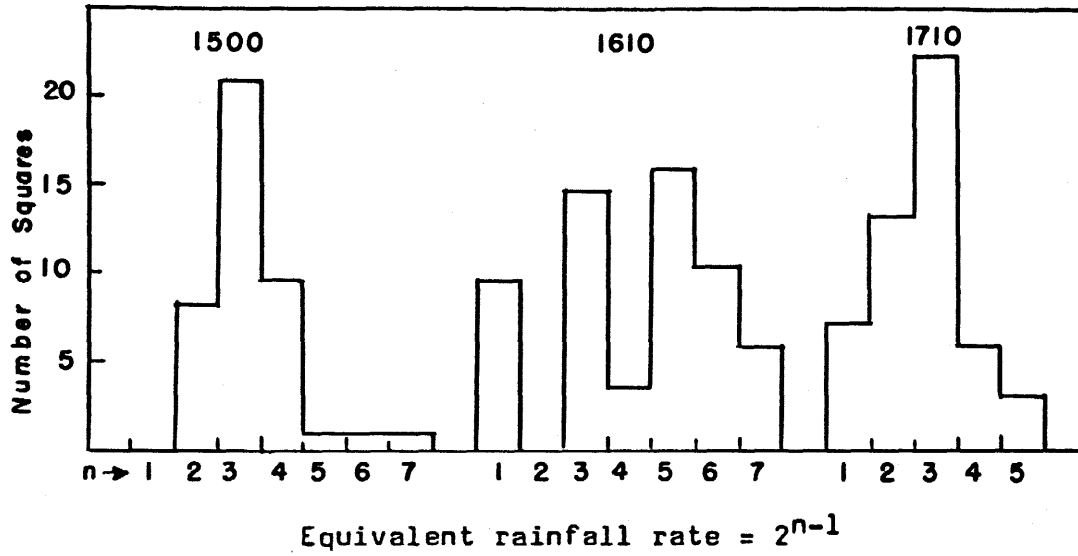
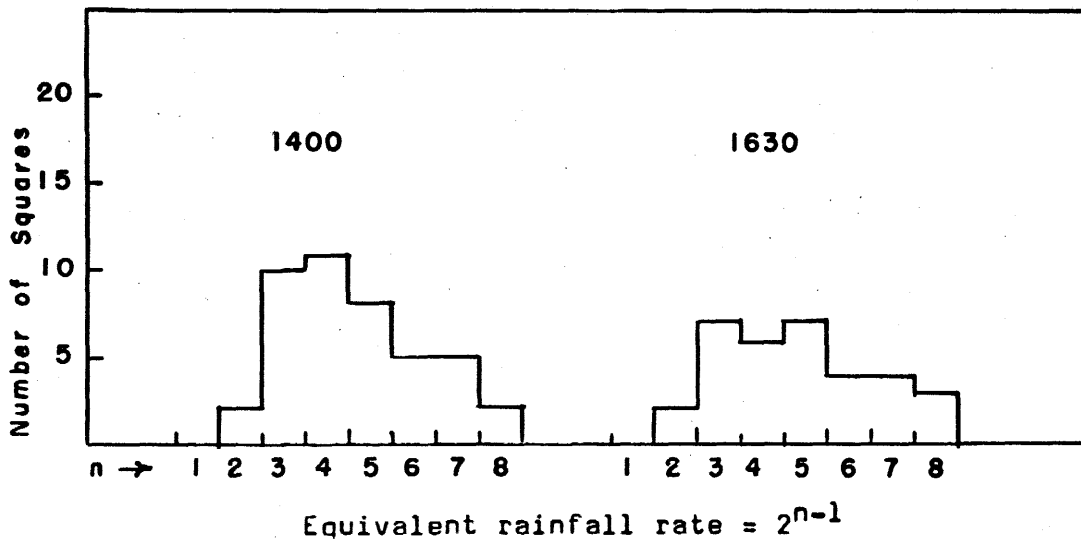


Fig. 18. Distribution of maximum hourly intensity over 80-mile circle for band storms.



14 June 63



26 July 62

Fig. 19. Examples of spatial intensity distributions in bands at selected times on 14 June 63 and 26 July 62.

B. Duration and Number of Bands

The information concerning storm duration and number of bands, peaks, etc., is summarized in Tables 8 and 9. Table 8 shows the total areal duration and actual band duration for each storm. The 22 storms which contained band patterns showed a tendency to be from six to 10 hours in total duration but ranged from six to 54 hours in length, as shown in Fig. 20. Because of the difficulty in comparing the length of storms consisting of only one band with storms consisting of a more complex structure, the duration of the actual band within the 80-mile circle was obtained, where possible, by use of both radar and rain-gauge data. Fig. 21 indicates these durations and shows a sharp peak at 6-7 hours. As far as could be determined, the values of actual band duration apply to each band alone.

The maximum total length of time a rain gauge received precipitation for an entire storm (Table 9) tended to be five to 10 hours with a range of four to 46 hours (Fig. 22). The maximum length of time a gauge received continuous precipitation was most often four to six hours with a range of four to 27 hours (Fig. 23). The rather odd distribution in Fig. 23 over the four to six hour range is possibly a result of the small sample of storms used in this study.

Four storms contained more than one band (see Table 8) and 16 storms, including three of the multi-band cases, contained one or more areas or spots in addition to the bands.

TABLE 8.
AREAL DURATIONS, NUMBER OF BANDS,
AND AREAL INTENSITY HISTOGRAM PEAKS FOR BAND STORMS

<u>Date</u>	<u>Total Area</u> <u>Duration (hours)</u>			<u>Band</u> <u>Duration</u> <u>(hours)</u>		<u>No.</u> <u>of</u> <u>Peaks</u>	<u>No.</u> <u>of</u> <u>Bands</u>
	6-13	14-20	>20	4-7	>7		
26-28 May 61			47	6		5	2
30 Oct-1 Nov 62			45	6		3	1
8 Jul 63			25	6		3	1
6-8 Nov 59			52		11	2	3
9 Jul 62	9			7		1	1
17 Aug 62		18			12	1	1
2 Jul 61		16			8	1	1
2-4 May 62			54		9	1	1
31 May 62	8			7		1	1
24 Jun 60		20		5		3	2
26 Jun 62	9			6		1	1
14 May 63	10			7		1	1
23 Oct 62		16		6		1	1
7 Aug 63	7			6		1	1
26 Jul 62		18		6		2	2
20 May 63	6			6		1	1
9-10 Oct 62			39	7		-	1
29-30 Jun 60			29	5		1	1
21 Jul 62	9			7		1	1
1 Aug 63	8				9	1	1
14 Jun 63	7			7		1	1
21 Jul 63		17		6		3	1
16 Nov 60							2
28 May 63							2

TABLE 9.

MAXIMUM DURATIONS AT ANY POINT WITHIN 80-MILE CIRCLE
FOR BAND STORMS

<u>Date</u>	<u>Maximum Point Total Duration (hours)</u>			<u>Maximum Point Continuous Duration (hours)</u>		
	1-10	11-25	>25	4-6	8-10	>10
26-28 May 61			46			24
30 Oct-1 Nov 62			41			27
8 Jul 63		20			10	
6-8 Nov 59			43			25
9 Jul 62	8			4		
17 Aug 62		17			8	
2 Jul 61		16			10	
2-4 May 62			36			17
31 May 62	7			6		
24 Jun 60		12		4		
26 Jun 62	7			4		
14 May 63	6			6		
23 Oct 62	9			6		
7 Aug 63	6			6		
26 Jul 62		14		6		
20 May 63	5			5		
9-10 Oct 62			36		9	
29-30 Jun 60		23		6		
21 Jul 62	4			4		
1 Aug 63	6			4		
14 Jun 63	4			4		
21 Jul 63		13		4		

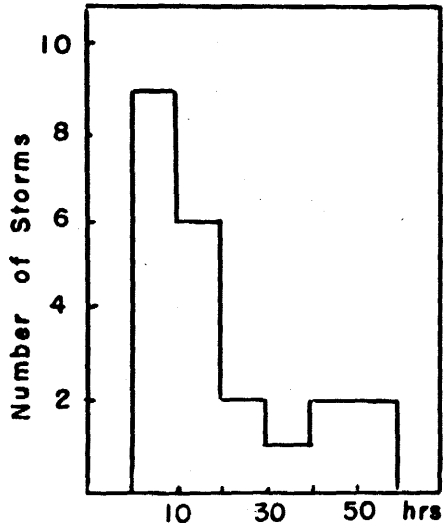


Fig. 20. Durations of entire storms.

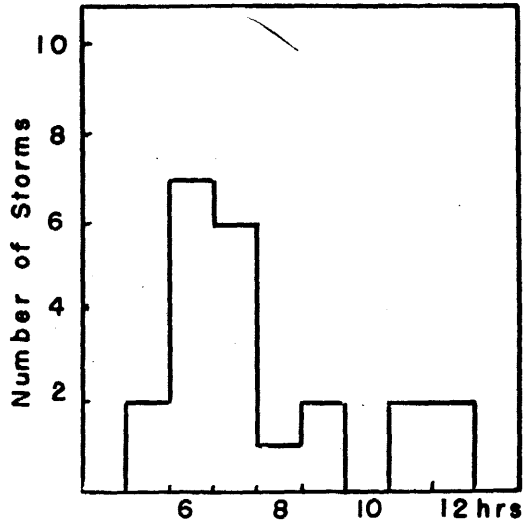


Fig. 21. Durations of single bands.

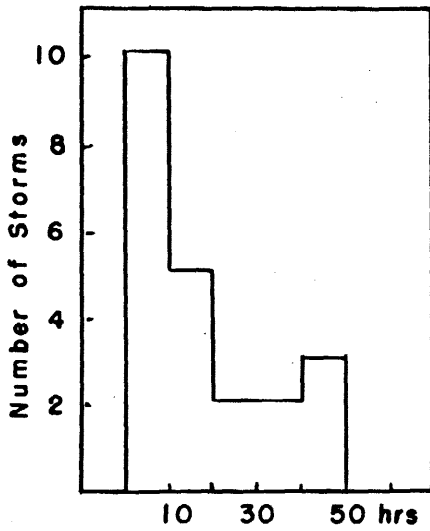


Fig. 22. Maximum total duration at a point within 80-mile circle.

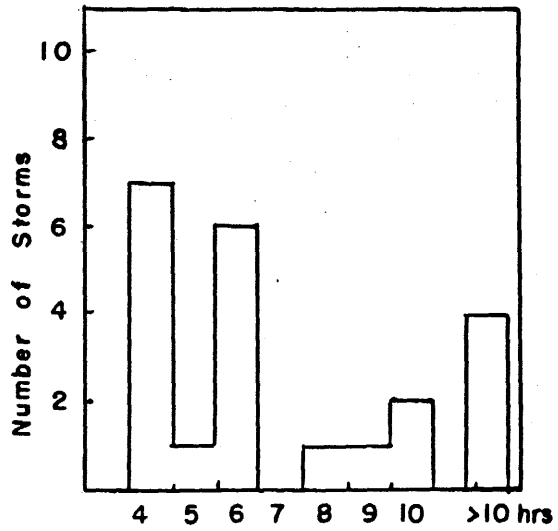


Fig. 23. Maximum continuous duration at a point within 80-mile circle.

Eleven of the latter storms had areas or spots before the band passage, whereas nine storms had areas or spots after the band passage. Four storms had areas or spots both before and after band passage. Of the 11 cases of areas preceding the band, nine had areas located over southwestern New England which lasted, in six storms, from five to 10 hours, and in the other three storms from 18 to 24 hours. Of the nine cases of areas following the band passage, three had areas over southwestern New England, three had areas over northern New England (mountains of Vermont and New Hampshire), two had light areas over the entire network of gauges, and one case had a light area that moved from west to east across Massachusetts. The duration of the areas which followed the band passage ranged from two to 45 hours with no particular relation between duration and location.

In a number of storms (7) more than one peak was reached in the total areal intensity histograms (see Table 8). Fig. 24 shows a histogram with several peaks. The peaks ranged in number from two to five and were, in most cases, directly associated with band and area passage through the 80-mile circle. Thus, in the histogram for 26-28 May 61, there are five peaks: two associated with two bands in succession, and three associated with three areas that followed the last band. However, the storm of 6-8 November 59 had two peaks: the first peak associated with three lines which passed in close succession, and the second peak associated with an area and spots following the bands. In most of the storms there exists

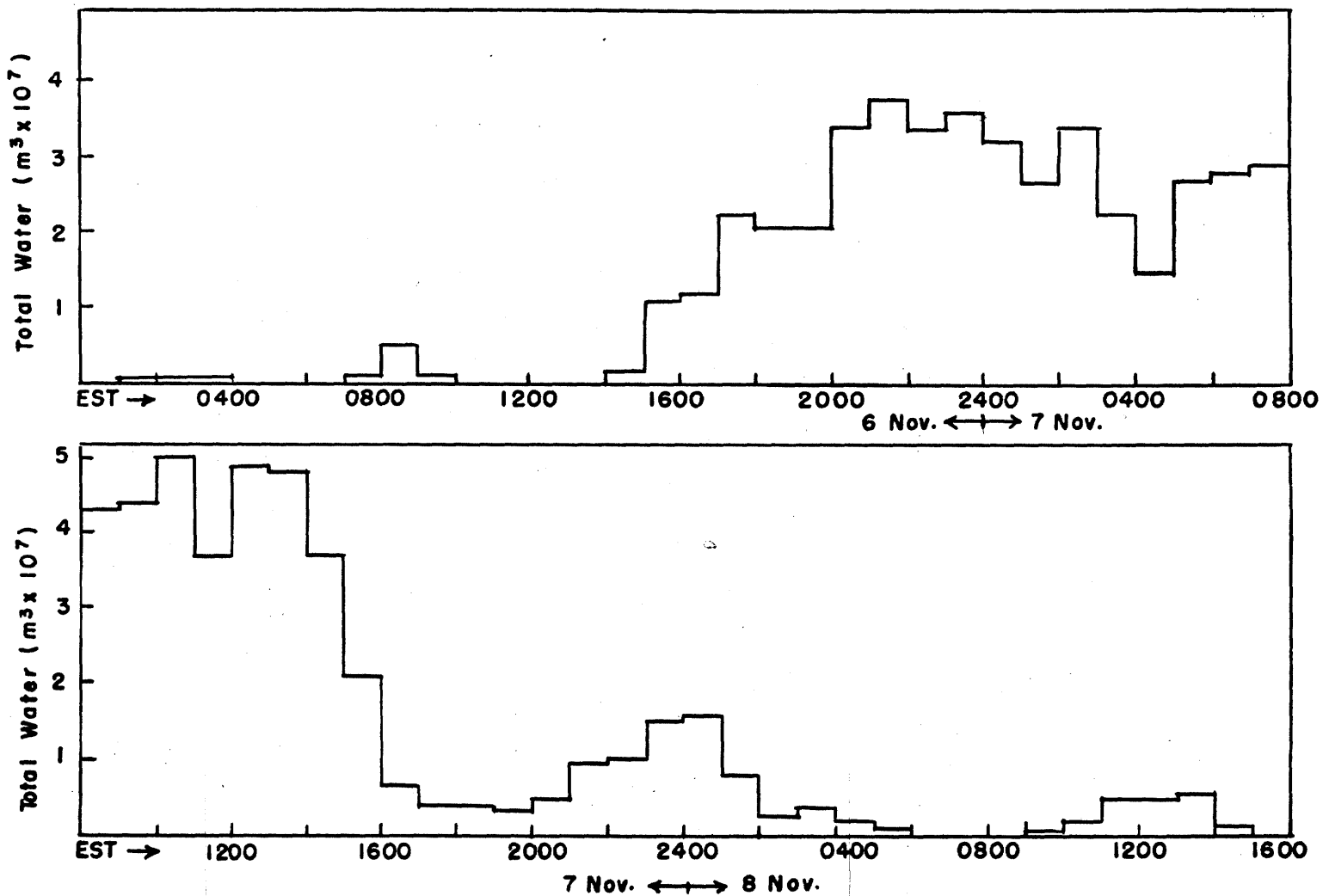


Fig. 24. Histogram of hourly areal intensity (total deposit within 80-mile circle) for 6-8 November 59.

one peak on the histogram that corresponds closely with the passage of one band through the 80-mile circle.

C. Band Dimensions

The results of an analysis of the dimensions of the 27 bands (four storms had more than one band) are shown in Table 10. The information was taken primarily from the radar data since the radar has better spatial and temporal resolution than the rain-gauge network. The dimensional values determined for each storm are rather approximate in nature.

The band length, insofar as the radars were able to detect it, varied from 80 to 195 miles with the largest group (13) having lengths of 100 to 150 miles. Nine bands were longer than 150 miles and five were shorter than 100 miles. Fig. 25 represents the distribution of band lengths and shows a distinct peak at 140-160 miles. In three storms which contained two bands the first band was the shorter; in the storm of 6-8 November 59 which contained three bands the first band was the longest and the last band was the shortest. All five of the storms that had bands less than 100 miles in length contained additional precipitation areas or spots either before or after the band passage.

The band width was more difficult to determine than the length since the width may vary considerably along the band and also may vary with time. In this study the values

TABLE 10.
BAND DIMENSIONS* AND ORIENTATION

<u>Date</u>	<u>Maximum Length (miles)</u>			<u>Maximum Width (miles)</u>			<u>Orien- tation</u>
	<100	100-150	>150	20	30	>39	
26-28 May 61	100	135		20			NE-SW
30 Oct-1 Nov 62	95			20			N-S
8 Jul 63		140			25		NE-SW
6-8 Nov 59		115 110			25	40	NE-SW
	80			15			
9 Jul 62			160	15			NE-SW
17 Aug 62			180			40	NE-SW
2 Jul 61			170		25		NE-SW
2-4 May 62		100			25		N-S
31 May 62			155	15			NE-SW
24 Jun 60			165 190		30 25		NE-SW
26 Jun 62		100		15			NE-SW
14 May 63		140		20			NE-SW
23 Oct 62		140			30		NE-SW
7 Aug 63			195			40	NE-SW
26 Jul 62		120 140		10		30	NE-SW
20 May 63			155		30		NE-SW

* Two or more values for each storm indicate more than one band. Top value is for band of earliest occurrence.

TABLE 10. (Continued)

<u>Date</u>	<u>Maximum Length (miles)</u>			<u>Maximum Width (miles)</u>			<u>Orien- tation</u>
	< 100	100-150	> 150	20	30	> 39	
9-10 Oct 62	95			20			NW-SE
29-30 Jun 60		150				40	NE-SW
21 Jul 62	90			15			NE-SW
1 Aug 63			170			60	N-S
14 Jun 63		150			30		NW-SE
21 Jul 63		145		15			NE-SW
16 Nov 60		130 150		20		30	NE-SW
28 May 63		125		20			NW-SE
			160		30		

* Two or more values for each storm indicate more than one band. Top value is for band of earliest occurrence.

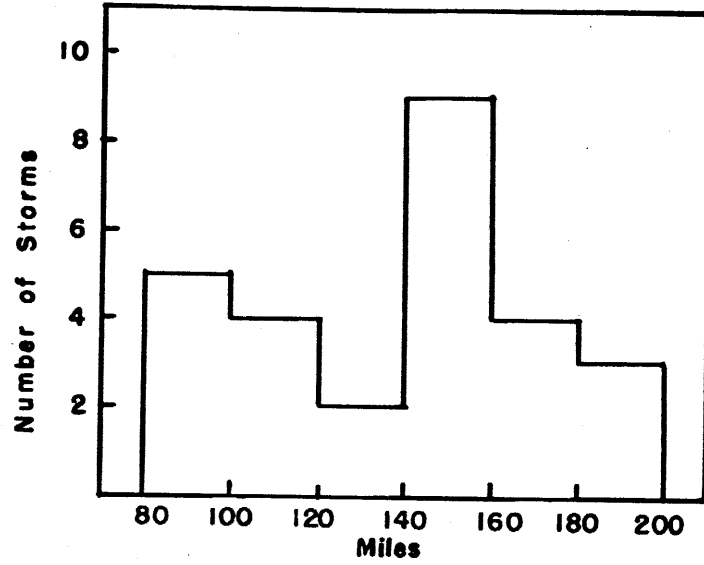


Fig. 25. Distribution of band lengths.

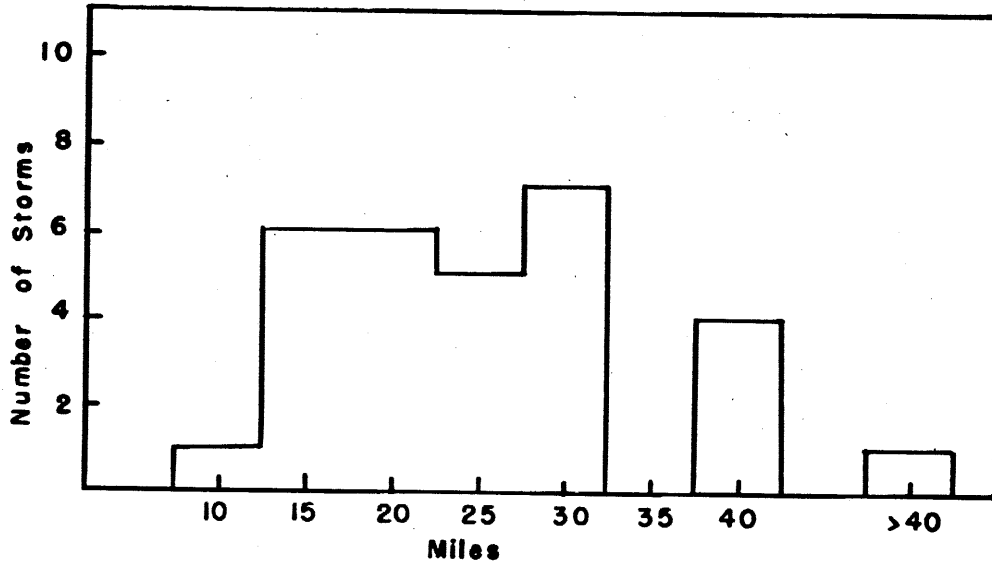


Fig. 26. Distribution of band widths.

presented represent the maximum width at any point along the band that was generally maintained as the band moved across the 80-mile circle. Fig. 26 represents the band distribution with width. The majority (17) of the cases fall into the 10 to 25 mile range with 10 of these having a maximum width of 20 to 25 miles. Nine bands range in maximum width from 30 to 60 miles.

The orientation of the bands was predominantly northeast to southwest (21 cases). However, four bands were oriented north-south and two were oriented northwest-southeast. In three of the multi-band situations the bands within the group maintained the same orientation; in the fourth case, 24 June 60, the first and shorter band was oriented north-south while the second and longer band was oriented northeast-southwest.

D. Cause of Precipitation

This study indicates that the most frequent cause of band-type precipitation in the New England area is the cold front. Table 11 shows the various causes of the band patterns as determined from the synoptic data. Twelve cases of bands were associated with cold fronts, five with occluded fronts, two with stationary fronts, one with a coastal low, and two cases were not associated with any particular disturbance. The last two cases were designated air mass showers. In two cases the bands were definitely prefrontal in nature: 2 July 61 was a pre-cold front band and 26 July 62 was a

TABLE 11.
SYNOPTIC DATA FOR BAND STORMS

<u>Date</u>	<u>Cause of Precipitation</u>						<u>Re Adj.</u>
	CF	WF	DF	SF	CL	Other	
26-28 May 61	x						
30 Oct-1 Nov 62			x				2
8 Jul 63			x				
6-8 Nov 59	x						4
9 Jul 62	x						
17 Aug 62	x						
2 Jul 61	x						
2-4 May 62			x				
31 May 62						Air Mass	
24 Jun 60	x						
26 Jun 62	x						
14 May 63	x						
23 Oct 62			x				4
7 Aug 63	x						
26 Jul 62			x				
20 May 63	x						
9-10 Oct 62					x		
29-30 Jun 60	x						
21 Jul 62	x						
1 Aug 63				x			
14 Jun 63						Air Mass	
21 Jul 63				x			
16 Nov 60						Air Mass	
28 May 63						Air Mass	

pre-occluded front situation with two bands. It was not determined in the rest of the cases whether the precipitation occurred precisely during the frontal passage, but, with the exception of the air mass showers, the front was considered to be in the general area of the bands. The orientation of all the bands is roughly parallel to the associated front.

The 500 mb pattern was investigated for the two air mass shower cases to determine possible causes of the bands. In the case of 31 May 62 a deep 500 mb low pressure center existed over northern Labrador with a trough extending down over the Great Lakes. The orientation of the band was almost parallel to the axis of the trough. In the case of 14 June 63 a rather sharp 500 mb trough extended down over eastern New England. These upper air patterns may have created enough instability for showers to form, but a closer investigation would be required for any definite conclusions to be drawn.

Some discussion of the storms of longer duration is warranted here. A glance at Table 11 indicates that most (16) of the storms involving bands also had additional areas or spots of precipitation either before or after band passage. These additional areas usually prolonged the total duration of the storm to greater or lesser degree. As was done in the study of area patterns an arbitrary value of 30 hours was set as the lower boundary for long storms. Three of the five storms thus defined contained either a cold front or an occluded front which moved through New England from the west or northwest and partially merged with a coastal low which passed to

the southeast off Cape Cod (26-28 May 61, 30 October-1 November 62, 2-4 May 62).

The two remaining storms involved single systems that became stationary out to sea. In the case of 6-8 November 59 a cold front moved through New England causing several light bands on 6 November; as the front moved out to sea and became stationary, precipitation persisted in the New England area well into 8 November. On 9-10 October 62 a coastal low formed off Virginia and moved east out to sea and became stationary well off the coast causing precipitation to persist over most of New England for some time. The band in this storm was very light and was not associated with any frontal activity. In all five of the long storms light areas and spots of precipitation persisted for many hours after the band passage over parts of New England, particularly in the mountainous regions.

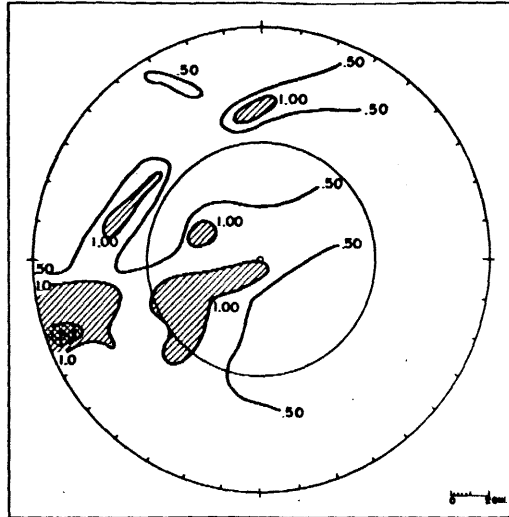
E. Spatial Distribution of Total Water

The results of an analysis of the rain-gauge maps of the total amount of water deposited by the entire storm are found in Table 12 which is similar to Table 6 for the areas. Considerable variation was found in the pattern of the spatial distribution of the total water. Some examples for the 12 cold fronts are in Fig. 27. Typically, there was an area or band of greater precipitation amounts which may be located either across the center of the circle, to the south or southeast, or well to the northwest. Some of the

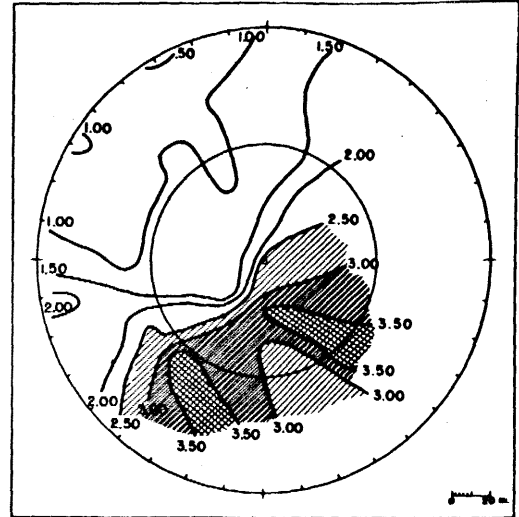
TABLE 12.

SPATIAL DISTRIBUTION OF TOTAL WATER IN BAND STORMS

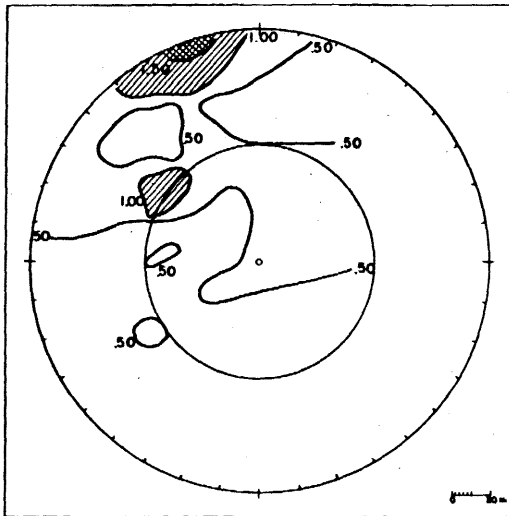
Date	Location of Heaviest Precip. Center			Precip. Cause	Highest Amount (in.)	Lowest Amount (in.)	Ratio
	S-SE	Band	Other				
26-28 May 61	x			CF + CL	3.68	.46	8.0
30 Oct-1 Nov 62	x			OF + CL	2.99	.88	3.4
8 Jul 63			x	OF	2.40	.00	--
6-8 Nov 59		x		CF → SF	1.99	.25	8.0
9 Jul 62	x			CF	1.80	.02	90.0
17 Aug 62		x		CF	1.75	.00	--
2 Jul 61			x	CF	1.85	.00	--
2-4 May 62			x	OF + CL	.97	.09	10.8
31 May 62		x		AM	1.41	.00	--
24 Jun 60			x	CF	2.03	.02	101.5
26 Jun 62		x		CF	.52	.00	--
14 May 63		x		CF	.85	.02	42.5
23 Oct 62	x			OF	.53	.04	13.2
7 Aug 63		x		CF	1.56	.00	--
26 Jul 62	x			OF	1.36	.00	--
20 May 63		x		CF	.79	.00	--
9-10 Oct 62	x			CL	.76	.00	--
29-30 Jun 60		x		CF	1.04	.00	--
21 Jul 62	x			CF	.74	.00	--
1 Aug 63			x	SF	1.13	.00	--
14 Jun 63			x	AM	.81	.00	--
21 Jul 63			x	SF	.72	.00	--



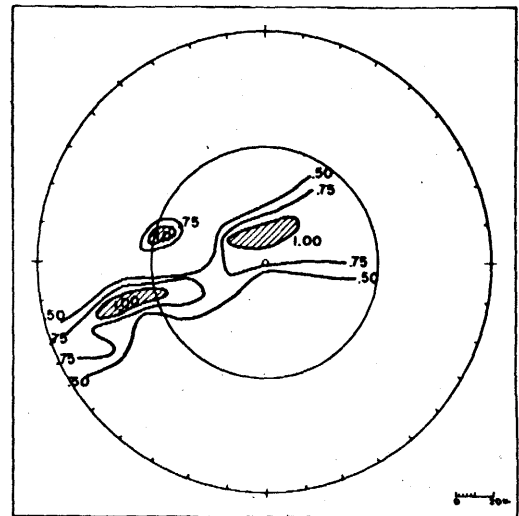
Cold front
17 August 62



Cold front + coastal low
26-28 May 61



Cold front (pre-frontal)
2 July 61



Air mass showers
31 May 62

Fig. 27. Spatial distributions of total water for some band storms.

storms had additional relatively heavy areas or spots in other regions but these appeared to be less dominant than the previous ones mentioned above. Two cases of areas in the far northwest may represent northward displaced bands that the rain-gauge network cannot define.

The remaining 10 storms, consisting of occluded fronts, stationary fronts, air mass showers, and a coastal low, showed patterns that were quite diverse in nature. There were six storms involving occluded fronts, a coastal low, or a combination of the two. In four of these there were areas of heavy precipitation to the southeast; in the other two there was a relatively heavy band to the north and northwest. The two stationary front patterns both had heavy areas to the far west. The two air mass shower patterns were somewhat similar in that they both exhibited band-like structure (Fig. 27) but they differed in orientation and extent.

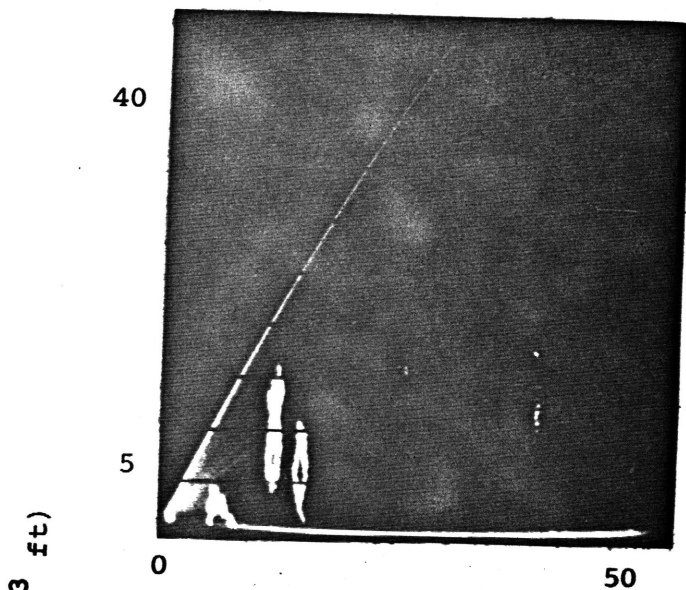
The highest and lowest values of total water received by any gauge within the 120-mile circle are noted in Table 12 for each storm. The ratio of the two values was computed, where possible. Clearly, the values fluctuated widely, and in many cases there were regions that received no precipitation at all.

F. Special Cases

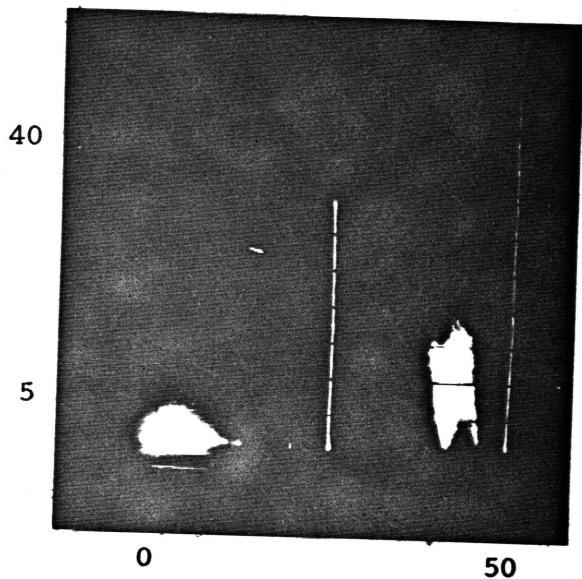
The bands of 16 November 60 and 28 May 63 are different from the others considered in this study in that in each case the radar observed two successive bands which moved across the 120-mile area, yet the rain-gauge network reported no precipitation at all on these dates.

A comparison of the radar PPI echoes with those on the RHI and with the hourly teletype data suggests that the bands did contain precipitation. Fig. 28 shows RHI photographs for both storms. In some places the echoes did not reach the surface during 16 November 60 whereas they definitely appeared to reach the surface on 28 May 63. Teletype data for 16 November 60 indicated that several stations received rain showers at the time the radar observed the bands over those stations. The same was true of 28 May 63. It was assumed that the rain either missed the gauges or the amounts were too small to be recorded. Since there are no rain-gauge data for these cases, all of the information concerning them must be inferred from the radar data.

The two storms are quite similar in most of their characteristics. Both storms were light in maximum point intensity with 16 November 60 having 15 mm/hr and 28 May 63 having 4 mm/hr. The duration of the bands was about 3-5 hours. The computed total water was $2.0 \times 10^8 \text{ m}^3$ for 16 November 60 and $1.2 \times 10^8 \text{ m}^3$ for 28 May 63, which puts them down near the bottom of the list. The band lengths are similar (see Table 8),



16 Nov 60 (1510 EST, 303°)



28 May 63 (1708 EST, 251°)

Fig. 28. Examples of photographs of AN/CPS-9 RHI echoes taken on 16 November 60 and 28 May 63.

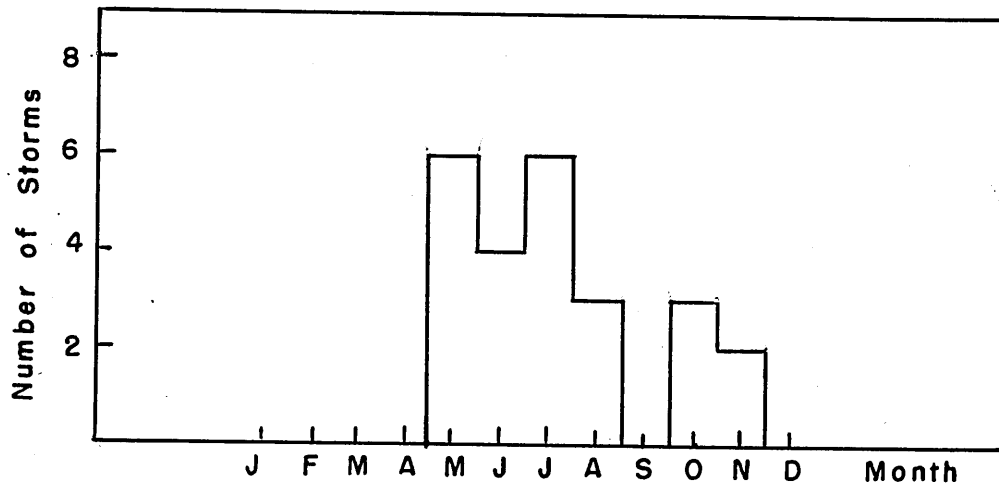


Fig. 29. Seasonal distribution of band storms.

but their orientations are different, being northeast-southwest for 16 November 60 and northwest-southeast for 28 May 63. Both storms must be considered air mass showers since there were no recognizable surface synoptic features in the vicinity. However, a fairly deep 500 mb trough existed over the Great Lakes on 16 November 60, and a local 500 mb trough existed just to the east of New England on 28 May 63. Little more can be said at this time about these two storms. They appear similar to the other bands in this study in their characteristics with the exception that no precipitation was detected by the rain-gauge network. The larger survey now in progress may pick up similar cases.

G. Seasonal Distribution

Fig. 29 shows the seasonal distribution of the storms containing band patterns. Most of the storms occurred in May through July, indicating that late spring and early summer may be the time when the development of intense convective bands is favored. The five storms that occurred in October and November contained bands of rather light precipitation (maximum point intensity was 15 mm/hr or lower) in contrast to those band cases occurring in May through July (maximum point intensity up to 250 mm/hr). In four of the five fall season cases precipitation areas existed in addition to the band patterns, and the intensity of these areas was generally equivalent to that of the associated band.

V COMPARATIVE CHARACTERISTICS OF STORMS WITH
PRECIPITATION AREAS, BANDS, OR MISCELLANEOUS PATTERNS

A. Miscellaneous Storms

The two groups of storms in this study were selected primarily on the basis of containing well defined areas or bands of precipitation. For comparison, some investigation was also made of storms which contained a moderate amount of precipitation but no well defined pattern. Table 13 summarizes the information available on 12 such storms which shall be referred to as miscellaneous storms. The characteristics included in the table are total water, maximum areal intensity, total areal duration, and precipitation cause.

With the exception of two cases, the storms containing miscellaneous patterns were rather low in total water deposited within the 80-mile circle and had somewhat low maximum areal intensities but were generally long in total duration. Values of total water ranged from 2×10^8 to less than $7 \times 10^8 \text{ m}^3$, whereas values of the maximum areal intensity varied from about 2×10^7 to $12 \times 10^7 \text{ m}^3$. On the other hand, the length of the storms varied rather widely from 12 to 56 hours in total duration. The two exceptional cases, particularly 4-7 October 62, exhibited unusually high total water and relatively large maximum areal intensity as well as being two of the three longest storms in this group. The extremely

TABLE 13.

CHARACTERISTICS OF STORMS CONTAINING MISCELLANEOUS PATTERNS

<u>Date</u>	<u>Total Water ($m^3 \times 10^8$)</u>	<u>Maximum Areal Intensity ($m^3/hr \times 10^7$)</u>	<u>Total Duration (hours)</u>	<u>Precip. Cause</u>
4-7 Oct 62	51.4	16.7	72	CL + SF
5-6 Dec 62	19.0	16.4	43	CL + SF
13-14 Aug 63	6.4	10.5	36	land low
20-21 Sep 63	5.0	5.7	33	CF + SF
29-30 May 63	4.9	7.5	21	land low
16-18 Sep 63	4.0	2.7	56	CL
23-24 Jan 63	3.9	3.5	29	land low
9 Jun 63	2.6	12.1	12	CF + SF
2 Aug 63	2.6	5.0	19	SF + L
6-7 Sep 63	2.3	1.9	27	CL
19-20 Jul 63	2.1	2.5	15	CF + SF
29-30 Aug 63	1.9	4.4	15	land low

long duration of 4-7 October 62 clearly contributed to its high total water.

The causes of precipitation in these storms were varied but can be divided into three groups: (a) a combination of two synoptic systems - two cases; (b) the evolution of one system into another - four cases; and (c) the movement, sometimes slow, of a single low center through or near the New England area - six cases. The first group includes two situations in which a rapidly intensifying coastal low moving slowly up the Atlantic coast combined with a stationary front in northern New England to produce the two highest total water amounts of any storm considered in this study. In both cases a trough aloft existed to the west over the Great Lakes. The second group involved three cases of a cold front moving down over New England to become an east-west stationary front just to the south. The other storm in group (b) was caused by a weak low center which formed on a stationary front just to the south of New England and which subsequently moved northward over the area. The third group involved four storms where a low center from the Great Lakes or further south passed over New England spreading precipitation far in advance of the actual system and two storms where a coastal low approached and passed very slowly off the southern New England coast. On 16-18 September 63 the coastal low became nearly stationary off New Jersey for a full 24 hours before moving slowly to the northeast, and light precipitation persisted over New

England for more than two days. In most cases there existed or developed a weak trough aloft over the northeastern United States.

B. Summary of Characteristics of the Various Groups

In Table 14 characteristics of the storms of the three pattern types (areas, bands, and miscellaneous) are summarized. In the following sections they are compared and discussed.

C. Total Water

In all three groups the same order of magnitude of total water was involved, that is, 10^8 - 10^9 m³, or a depth of about 2-25 mm. The areas showed a fairly even distribution over this range, but both the bands and the miscellaneous storms indicated a preference for the lower values. Several of the storms containing bands deposited rather high amounts of water but this resulted from the contribution of additional precipitation areas rather than from the bands themselves. Also, two of the miscellaneous storms deposited exceptionally high amounts of water but their unusually long duration was considered to be a contributing factor.

The spatial distribution of total water was quite varied for both the area and the band groups. There were no particular configurations that were definitely characteristic of each group. However, whereas the area cases tended to deposit

TABLE 14.

CHARACTERISTICS OF STORMS CONTAINING PRECIPITATION AREAS,
BANDS, AND MISCELLANEOUS PATTERNS

<u>Characteristic</u>		<u>Areas</u>	<u>Bands</u>	<u>Misc.</u>
Total Water Deposited ($m^3 \times 10^8$)	* HF Range	none 1.5-11.8	0.4-2.0 0.4-16.5	2.0-6.5 1.9-51.4
Maximum Intensity at a Point (mm/hr)	HF Range	4-8 4-30	65-130 4-250	
Maximum Intensity over Total Area ($m^3/hr \times 10^7$)	HF Range	2-10 2-24	1-10 1-17	2.0-5.0 1.9-16.7
Total Area Duration (hrs)	HF Range	16-30 8-48	6-10 6-54	19-36 12-72
Principal Area Duration (hrs)	HF Range	8-23 8-46	6-7 5-12	
Maximum Total Duration at a Point (hrs)	HF Range	14-30 8-47	5-10 4-46	
Maximum Continuous Duration at a Point (hrs)	HF Range	10-24 6-30	4-6 4-27	
Precipitation Cause	HF Range	Coastal Low	Cold Front	
Seasonal Distribution	HF Range	Feb-Mar	May-Jul	Aug-Sep

* Highest Frequency

more amounts to the south or southeast (influence of the coastal lows), the band cases were more apt to deposit wide northeast-southwest bands of a greater depth through the center of the 120-mile circle. Other areas of greater depth for both groups were found to the northwest, west and southwest. In addition, the depth gradient was much steeper for the bands than for the areas. Almost all of the area storms deposited measurable amounts of water over the entire 120-mile circle, whereas the band storms often appeared to leave some regions completely dry.

D. Intensity

The area and band groups differ significantly with respect to the maximum point intensity. The areas most often contained maximum intensities of 4-8 mm/hr while the bands usually exhibited maximum intensities of 65-130 mm/hr. The maximum point intensity was computed in four of the miscellaneous storms and was found to vary widely from 15 to 65 mm/hr. It is clear that heavy precipitation is more likely to occur in bands than in areas.

Contrary to the maximum point intensities, the maximum areal intensity (hourly intensity over the entire 80-mile area) did not differ significantly with respect to the three groups. The indication is that the bands deposit greater amounts of water in smaller areas, whereas the area storms cover a larger region with smaller but more uniform amounts.

Fig. 30 shows one-hour rain-gauge patterns for an area storm (2 March 63) and for a band storm (9 July 62) that have similar total water for the hour (or hourly areal intensity) but which differ considerably in areal coverage and local intensity.

E. Durations

In general, the storms containing bands were definitely shorter than those containing areas or miscellaneous patterns. The precipitation associated with the bands themselves lasted only 6-7 hours within the 80-mile circle, whereas that of the areas and miscellaneous storms tended to persist for 20-30 hours. All three groups had a few storms which had exceptionally long durations, but in most respects they appeared to be rather heterogeneous. Most of the storms which were classified as bands but which had unusually long durations included precipitation areas or spots outside of the band pattern itself. Long duration of the area storms was caused in some cases by the persistence of very light precipitation in hilly or mountainous regions for many hours after the passage of the main area. The maximum total and continuous durations at a point are similarly longer for areas than for bands.

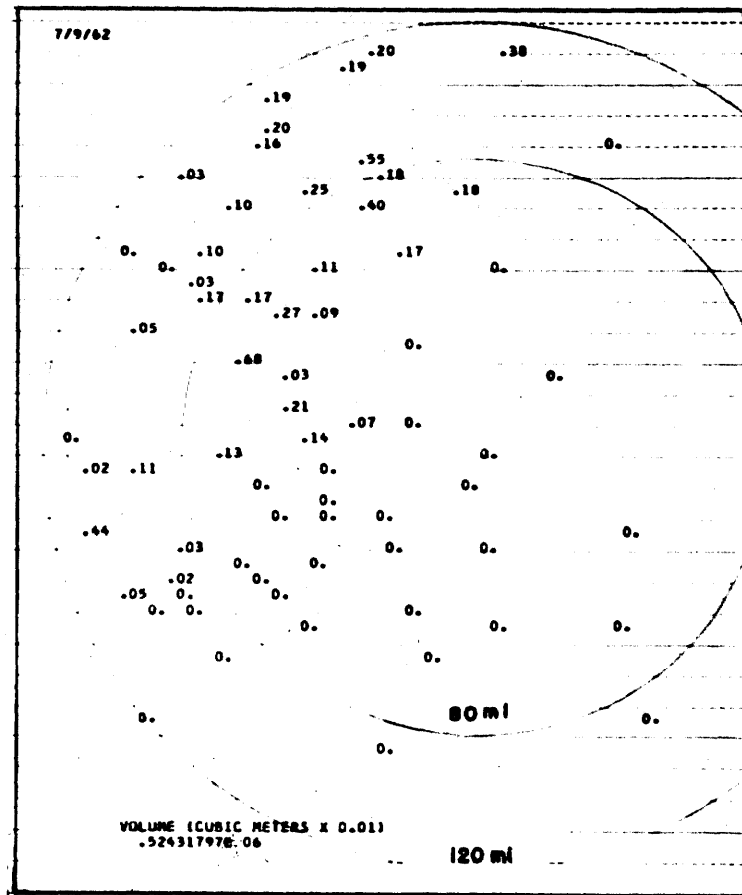
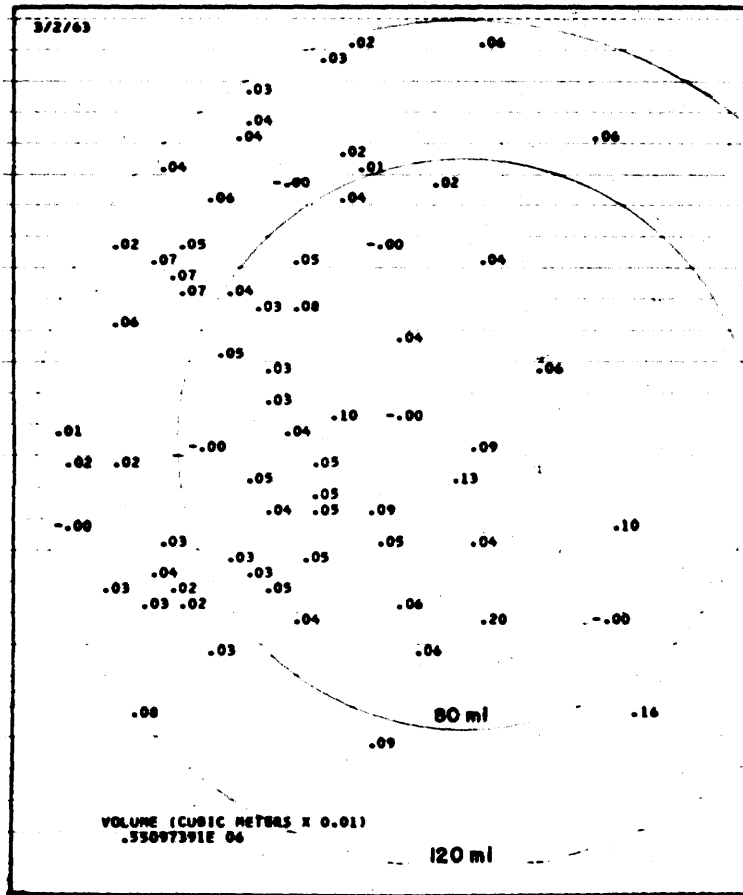


Fig. 30. One-hour rain-gauge patterns for 0100 EST, 2 March 63 and 1100 EST, 9 July 62.

F. Dimensions

It is difficult to make exact statements about the dimensions of areas of light intensity because they usually extended beyond the 120-mile circle for which rain-gauge data were plotted as well as beyond the range of radar detectability. For areas of 1-2 mm/hr, therefore, little can be said except that they are often over 200 miles in diameter. On the other hand, areas of 4 mm/hr or more were likely to be quite small, usually on the order of 30-40 miles across. Quite often the smaller intense areas were elongated with a northeast-southwest orientation.

In contrast to the area situations, the band dimensions were fairly well defined by the radar. The bands were usually 120-160 miles long and 15-30 miles wide. Occasionally, lengths of 200 miles and widths of 40 miles were reached but these appeared to be unusual. The bands, therefore, covered a much smaller portion of the 80-mile circle than did the areas.

G. Cause of Precipitation

The band and area groups differed significantly with respect to their associated larger-scale weather systems. Coastal lows were most often associated with the area patterns, whereas cold fronts were most often associated with band patterns. The miscellaneous patterns were often related to a combination of a stationary front and some other system.

In all three groups the longer storms tended to be related to complex situations which contained more than one frontal or low pressure system. Single frontal or low pressure systems, however, also were responsible for the long duration of some cases.

H. Seasonal Distribution

Finally, differences of some significance occur in the seasonal distributions of the three groups. Fig. 31 shows the relative distributions by month of the storms containing precipitation areas, bands, and miscellaneous patterns. Most of the area storms occurred in late winter, while the majority of the band storms occurred in late spring and early summer; half of the miscellaneous storms occurred in the late summer. From the above distributions it may be concluded that well defined areas occur most often in the late winter but, because the storms in this study were selected on the basis of radar pattern alone, little can be said about the predictability of any latewinter storm having an area pattern. Similar comments can be made for both the band and miscellaneous storms. A large sample of storms selected without consideration for radar pattern is necessary to determine a representative seasonal distribution.

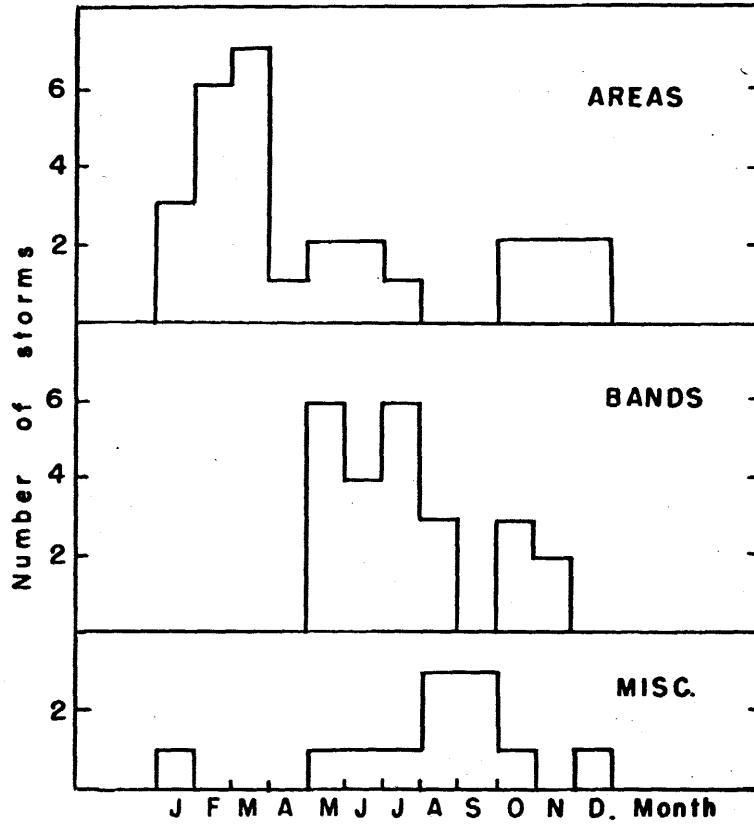


Fig. 31. Seasonal distributions of storms in area, band and miscellaneous groups.

VI CONCLUSIONS

In this study it was attempted to determine the general characteristics of mesoscale precipitation patterns in the central New England area. Sixty-four storms were selected on the basis of pattern as shown by 3 and 10 cm radars and then grouped according to area, band or miscellaneous pattern. Both radar and rain-gauge network data were used to determine for each storm the following quantities within a circle of radius 80 miles centered at Cambridge, Massachusetts: total amount of water deposited by the storm, maximum amount of water deposited during any single hour, maximum instantaneous precipitation rate at any point, total duration of precipitation, maximum duration of precipitation at any single point, and dimensions of precipitation areas or bands. In addition, the characteristics of the associated larger-scale synoptic systems and the spatial distribution of the total water were noted. The region under consideration, with a 100° sector omitted, has a total area of $4 \times 10^{10} \text{ m}^2$.

It was found that in the case of the area storms the rain-gauge data were more useful than the radar data for providing the desired information primarily because the radar range was limited in situations where precipitation at low levels predominated. On the other hand, in the cases of band patterns, the radar data were the most reliable, since the rain-gauge network was not dense enough to detect individual

storms in a representative way, and the radar range was less restricted in view of the greater vertical extent of the band patterns.

The results of this study indicate that there is no one factor that governs the total amount of water deposited within the observed area. In all the storms considered the total water was on the order of 10^8 - 10^9 m³ while the maximum hourly amounts were on the order of 10^7 - 10^8 m³. Somewhat larger amounts of total water are associated with the area storms which usually cover a larger region and last longer than the bands, even though the bands contain greater rainfall intensities. Exceptionally large amounts of water were received by two of the miscellaneous storms and were primarily a result of long duration. The spatial distribution of total water was quite varied for both the area and band groups but showed a tendency toward regions of greater amounts to the south in the area cases and toward wide northeast-southwest bands across the center of the circle for the band storms.

Maximum intensities at a point differed markedly between area patterns and band patterns, but maximum intensities over the entire 80-mile circle were quite similar for all three groups. The areas had maximum point intensities of 4-8 mm/hr in general whereas the bands most often had 65-130 mm/hr.

Precipitation in both the area and miscellaneous storms lasted significantly longer than that in the band patterns, being generally 20-30 hours in length as opposed to 6-7 hours

for the bands. Storms classified as bands, but which had large total water amounts and long durations, included a good deal of precipitation in the form of areas and spots in addition to the band patterns.

Light precipitation areas of 1-2 mm/hr were usually over 200 miles in diameter and thus could not be adequately defined by either the radar or the rain-gauge network used in this study; but the size of areas of 4 mm/hr or more was fairly easily defined to be generally of the order of 30-50 miles across or less. Bands were generally 120-160 miles long and 15-30 miles wide as indicated by the radar.

The major cause of precipitation in the area storms was the coastal low pressure center that passed to the southeast of New England while the major cause in the band storms was the cold front that moved across the New England area from the west or northwest. Storms of long duration and large amounts of deposited water were caused either by complex systems or a slow moving single system.

The seasonal distributions of the three groups of storms indicated that most of the area cases occurred in February and March while most of the bands occurred in May through July; the miscellaneous storms occurred with highest frequency in August and September.

The conclusions reached in this study can only be considered as tentative. The sample of storms in each pattern group was too small to be considered statistically but large enough to preclude thorough investigation of each one individually. The method of data selection, based upon radar pattern only may have introduced considerable bias. However, a study such as this one can be useful in guiding future research. Selection of the storms in the future should be based not only upon radar pattern but upon a combination of radar and rain-gauge data. A sample of storms which includes all storms over a period of a few years that deposited significant amounts of precipitation in the area should be selected. Such a sample would be independent of radar pattern. Larger samples must be used in each group so that statistics may be meaningful and truly representative. More consistency in radar operation should be obtained not only with respect to full temporal coverage of storms, but also with respect to the changing from one radar to another during the observation. A larger investigation of mesoscale precipitation patterns which is based in part on these suggestions is currently under way.

REFERENCES

- Austin, P. M., 1964: Radar measurements of precipitation rate, World Conference on Radio Meteorology incorporating the Eleventh Weather Radar Conference, A.M.S., Boston, 120-125.
- Austin, P. M., and S. Geotis, 1960: The radar equation parameters, Proc. of the Eighth Weather Radar Conference, A.M.S., Boston, 15-22.
- Battan, L. J., 1959: Radar Meteorology, The University of Chicago Press, Ill., pp. 54-55.
- Boucher, R. J., 1961: The motion and predictability of precipitation areas as determined from radar observations, Proc. of the Ninth Weather Radar Conference, A.M.S., Boston, 37-42.
- Boucher, R. J., and R. Wexler, 1961: The motion and predictability of precipitation lines, J. Meteor. 18, 2, 160-171.
- Cochran, H. B., 1961: A numerical description of New England squall lines, S.M. Thesis, Dept. of Meteor., Mass. Inst. of Technology, Cambridge, Mass., 25 pp.
- Fujita, T., 1963: Analytical mesometeorology: a review, Severe Local Storms, Meteorological monographs 5, 27, 77-125.
- Geotis, S., 1963: Some radar measurements of hailstorms, J. Applied Meteor. 2, 2, 270-275.
- Gunn, K. L. S., and T. W. R. East, 1954: The microwave properties of precipitation particles, Quart. J. R. Meteor. Soc., 80, 522-545.

- Kodaira, N., 1959; Quantitative mapping of radar weather echoes, Research Report Number 30, Weather Radar Research, Dept. of Meteor., Mass. Inst. of Technology, Cambridge, Mass., 39 pp.
- Marshall, J. S., and W. McK. Palmer, 1948; The distribution of raindrops with size, J. Meteor., 5, 165-166.
- Noel, T. M., and A. Fleisher, 1960; The linear predictability of weather radar signals, Research Report Number 34, Weather Radar Research, Dept. of Meteor., Mass. Inst. of Technology, Cambridge, Mass., 46 pp.
- Stem, T. F., 1964; Characteristics of New England thunderstorms viewed on 10 cm radar, S.M. Thesis, Dept. of Meteor., Mass. Inst. of Technology, Cambridge, Mass., 168 pp.
- Swisher, S. D., 1959; Rainfall patterns associated with instability lines in New England, S.M. Thesis, Dept. of Meteor., Mass. Inst. of Technology, Cambridge, Mass., 33 pp.
- Taylor, H. E., 1962; An investigation of the efficiencies of the stratiform and cellular modes of precipitation, S.M. Thesis, Dept. of Meteor., Mass. Inst. of Technology, Cambridge, Mass., 48 pp.